Interference-Optimal Frequency Allocation in Femtocellular Networks

by

Mahmoud Ouda

A thesis submitted to the
School of Computing
in conformity with the requirements for
the degree of Master of Science

Queen's University
Kingston, Ontario, Canada
March 2012

Abstract

The evolution of Mobile Internet has led to the growth of bandwidth demanding applications like video streaming and social networking. The required data rates projected for such applications cannot be sustained by current cellular networks. New network architectures like Long Term Evolution (LTE) and LTE Advanced have been carefully engineered and introduced to fulfill such large data rates.

The recent introduction of femtocells enabled high data rates and better coverage indoors, without the need for site establishment or upgrading the network infrastructure. Femtocells, however, will potentially suffer from major interference problems due to their expected dense and ad hoc deployment. The main contribution in this thesis is the introduction of a new and a very promising direction in deriving capable and efficient interference mitigation schemes, and comparing this direction to current techniques in the literature. Several works have studied the effect of interference on networks employing femtocells. In this thesis, we also survey such works and provide an overview of the elements considered in mitigating interference.

We introduce a new scheme known for its optimality, and use it for frequency assignment in downlink femtocell networks. The algorithm is based on optimization search rather than greedy or heuristic methods. Experimental simulations will be shown to evaluate the proposed scheme against other schemes from the literature.

Acknowledgments

The work presented in this thesis is conducted as part of the Masters program of the School of Computing at Queen's University, under the supervision of Dr. Hossam Hassanein, and the co-supervision of Dr. Najah Abed AbuAli. A portion of this work was supported by QUWIC (Qatar University Wireless Innovations Center).

I would like to thank Dr. Hossam Hassanein, from the School of Computing at Queen's University, for providing me with the opportunity to study at Queen's. Dr. Hossam have demonstrated a unique example of how a supervisor - as professional as he was - could be a close friend. Despite being a Computer Science graduate, I have been fit smoothly in a Telecommunications Research Lab. I knew this would have been a challenge for Dr. Hossam and myself, but the way I was fit in this lab was just right.

I would also like to acknowledge the efforts of Dr. Najah from the College of IT at UAE, towards the achievement of this thesis. Dr. Najah have been co-supervising my thesis since the early stages, and despite the time zone difference, she was able provide guidance and she was flexibly available for clarifications.

I extend my thanks to Dr. Abd-Elhamid Taha from the School of Computing at Queen's University, for reviewing and providing feedback on all document artifacts that have been used in this thesis. Dr. Taha is an example of a relentless, patient

coach. I thank him for his enormous efforts and invaluable advices on the professional and personal level.

In addition, I would convey my gratitude to my friends and family in Egypt, who supported my decision to study abroad. Also, I would like to thank all my friends in the Telecommunications Research Lab and School of Computing, who have been constantly providing me with advices and whom I have spent unforgotten times with them. I do remember people who stood beside me at the hard times, Abdulmone'm, Dina, Gehan, Hatem, Khalid, Layan, Mervat, Qutqut, Sharief, Shereen, and Walid.

Finally, I cannot express how much gratitude I owe my fiancée, Samar, who have been there for me since day one. She showed extreme support throughout the duration of my study, and was holding up really well, even at the toughest times when I was away. Thank You!

Contents

List of Tables

List of Figures

List of Acronyms

1G	First Generation
2G	Second Generation
3G	Third Generation
3GPP	3rd Generation Partnership Project
3GPP2	3rd Generation Partnership Project 2
4G	Fourth Generation
ACI	Adjacent Channel Interference
ASE	Area Spectral Efficiency
BS	Base Station
BSC	Base Station Controller
CAPEX	CAPital EXpenditure
CCI	Co-Channel Interference
CDMA	Code Division Multiple Access
CI	Computational Intelligence
CoI	Cell of Interest
CSG	Closed Subscriber Group
DAS	Distributed Antenna Systems
DCA	Dynamic Channel Allocation
DFS	Dynamic Frequency Selection
DSL	Digital Subscriber Line
eNB	eNode B
FAP	Femtocell Access Point
FBS	Femtocell Base Station

FCA	Fixed Channel Assignment
FFR	Fractional Frequency Reuse
FUE	Femtocell User Equipment
GA	Genetic Algorithm
GoS	Grade of Service
GPRS	General Packet Radio Services
GSM	Global System for Mobile Communications (Groupe Spécial Mobile)
HCA	Hybrid Channel Allocation
HeNB	Home eNode B(femtocell)
HetNet	Heterogeneous Network
IEEE	Institute of Electrical and Electronics Engineers
ILCA	Interference Limited Coverage Area
ISI	Inter-Symbol Interference
LP	Linear Programming
LTE	Long Term Evolution
MAC	Medium Access Control
MBS	Macrocell Base Station
MCF	Minimum Cost Flow
MDRP	Maximal Dynamic Reuse Partitioning
MUE	Macrocell User Equipment
NN	Neural Network
ODRP	Optimal Dynamic Reuse Partitioning
OFDMA	Orthogonal Frequency Division Multiple Access
OFDM	Orthogonal Frequency Division Multiplexing

OPEX	OPerational EXpenditure
OSG	Open Subscriber Group
PDF	Probability Density Function
QoS	Quality of Service
RB	Resource Block
RRM	Radio Resource Management
RSSI	Received Signal Strength Indicator
RWP	Random Waypoint
SA	Simulated Annealing
SI	Swarm Intelligence
SINR	Signal to Interference and Noise Ratio
SIR	Signal to Interference Ratio
SMS	Short Message Service
UE	User Equipment
VoIP	Voice over IP
WCDMA	Wideband Code Division Multiple Access
WiMAX	Worldwide Interoperability for Microwave Access

Chapter 1

Introduction

The cellular market has always been a demanding, ever evolving market. Since the introduction of mobile phones in the early 1990s, digital mobile phones have grown to reach around 5 billion subscriptions worldwide, around 76% of the world population [1]. In parallel, the Internet has been also growing, to reach 1.6 billion users worldwide, nearly 25% of the world population [2]. Blogs, social networks, video streaming and video gaming are continuously pushing the Internet traffic to its limits.

The current cellular systems started evolving since the 1980s. The introduction of First Generation (1G) mobile networks aimed at providing voice only services. It was based solely on analog technologies. The 1G systems have been replaced soon by Second Generation (2G) digital mobile systems. The primary data services introduced in 2G were Short Message Service (SMS) and circuit-switched data services [3]. This enabled e-mail and other data applications to rise and opened a huge amount of market opportunities for cellular operators and application development. Post the mid 1990s, packet data has become a reality with the introduction of General Packet Radio Services (GPRS) in Global System for Mobile Communications (GSM) networks,

referred to as 2.5G.

The introduction of Third Generation (3G) mobile services [3] has merged both the digital mobile technology and the Internet technology. This merging boosted both markets promoting the fact that consumers are getting too attached to their mobile phones and increasing their hours of stay online. This also expanded the market for new bandwidth demanding applications that encourage more mobile usage.

The current specifications of Fourth Generation (4G) wireless cellular standards promise hundreds of Mbit/s that should reach up to 1 Gbit/s for low mobility communications. With the ever increasing number of mobile users in the same territory, these rates might be difficult to achieve without optimized signaling, modulation, coding and interference resistance mechanisms. Nowadays, an emerging trend has been put into action to virtually extend the territory covered by a certain provider, which is: layering cellular networks, resulting in the formation of small cells within larger cells, as in Figure 1.1. This kind of reusing the physical space, enhances what is known as the Area Spectral Efficiency (ASE) [4, 5]. The ASE of a cellular system can be defined as the achievable throughput per unit area for the available bandwidth [6]. Since shrinking the cell size is the simplest and most effective way of increasing wireless throughput [7, 8], hence, was the introduction of indoor base stations forming picocells and recently femtocells [9]. The introduction of these small coverage networks requires also optimized operational mechanisms in order to co-exist with larger macrocell networks.

Typically, femtocells form a coverage area that layers the macrocell coverage area. The two layers share the physical space, and form smaller cells that provide indoor coverage within the vicinity of larger cells, as shown in Figure 1.1. Femtocells are

expected to have a very strong penetration rate at homes, offices and malls. End users will install their Femtocell Base Stations (FBSs) on their own. FBSs installation will be done in a convenient plug and play manner, and hence, non-coordinated ad-hoc deployment is inevitable. Such deployment is more likely to introduce interference [10], which will adversely affect the capacity of the radio system in addition to the quality of the individual communication links. Capacity increase is fundamentally the result of a trade-off between interference and quality, and hence, there is a need for interference management techniques to minimize interference which might otherwise counteract the capacity gains and degrade the quality of the network.

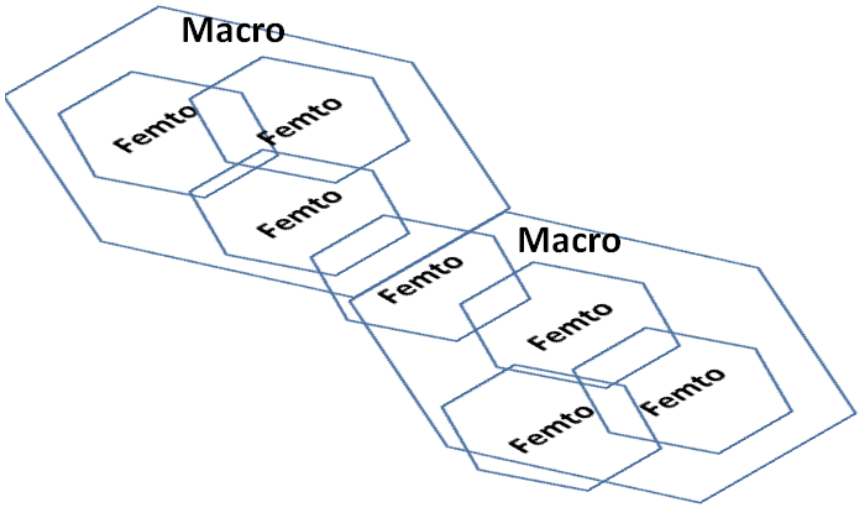

Figure 1.1: Illustration of a two tiered network, with femtocells ad-hoc deployment.

1.1 Motivation

Femtocells have been attracting much attention recently as a solution to the problem of poor cellular indoor coverage and capacity. With the estimation that 2/3 of calls and over 90% of data services occur indoors [9], besides, 45% of households and 30%

of businesses experience poor indoor coverage [11], the importance of indoor coverage emerges. Providing a reliable and strong indoor coverage of voice as well as video and high speed data services will soon be a must for mobile operators to survive. To emphasize on the rising importance of data, table 1.1 shows the growth of operator revenues for leading operators in Q3 2007, relative to the previous 12-month period, just before the femtocell technology started to appear. It can be noticed that some operators did not even grow positively in terms of voice revenue and that data revenue growth was more dominant. One of the obvious reasons of the significant drop in voice revenue is Voice over IP (VoIP) which enabled voice calls at relatively very low cost compared to cellular operators.

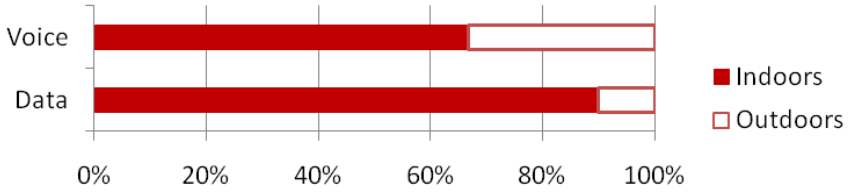

Figure 1.2: Percentage of indoor to outdoor voice and data sessions. Reproduced from [9]

With all what preceded in mind, and given the cost of establishing a Base Station (BS); a cheaper and more effective solution is preferred. Femtocells are expected to substantially reduce the operator CAPital EXpenditure (CAPEX) and OPerational EXpenditure (OPEX) [12, 13], which explains the great interest shown by cellular operators deploying femtocells. UMTS FBSs are expected to reach 70 million devices installed indoors, serving more than 150 million users [14], which is clearly why experts think that femtocells represent a promising direction from the operator economic view.

Femtocells are expected to offload much traffic to indoors, freeing resources at the macrocells and helping outdoor users to gain better user experience, providing at the

Mobile Operator	Data revenue growth	Voice revenue growth
AT&T	64%	6%
Verizon Wireless	63%	7%
Rogers	53%	15%
Telstra	50%	5%
Vodafone (W. Europe)	45%	1%
Sprint	28%	-9%
T-Mobile Germany	24%	-4%
KDDI	18%	1%

Table 1.1: Growth of operator revenues for leading operators in Q3 2007, relative to the previous 12-month period. [16]

same time a very rich user experience for indoor users without any special equipment apart from the FBS, and without any upgrades to their current handsets [15].

1.2 Problem Context

Due to their wireless nature, femtocell networks are subject to varying levels and types of interference [17]. Adding to that the characteristic of ad-hoc deployment, which might elevate interference to unbearable levels, rendering the network inefficient [18] and sometimes unusable. The distributed nature of the problem makes it even more challenging [19]. Several works were targetted towards interference mitigation, candidates of such works are surveyed in section 2.6.

This thesis targets interference mitigation in femtocell environments. While different techniques can be used for interference mitigation, frequency allocation comes as the interference mitigation technique of choice in this thesis. The method proposed in this thesis can be used in quite numerous scenarios. However, we chose frequency allocation in networks employing Orthogonal Frequency Division Multiple

Access (OFDMA) in their downlink, as it is the multiple access scheme utilized in emerging networks such as LTE, LTE-Advanced WiMAX.

In this thesis an optimal assignment solution is presented. It will be used as a benchmark to other schemes from the literature. Towards the end of this thesis, the tradeoff between performance and complexity will be discussed, and recommendations will be presented.

One major challenge that is addressed in this thesis, is the simulation environment. The femtocellular setup differs from the regular macrocell setup in two important aspects: 1. The network size, and 2. The ad-hoc nature of the setup. Chapter 4 shows how simulation challenges were addressed and what assumptions have been considered.

1.3 Contribution

The contribution in this thesis can be summarized in the following points:

1. Incorporating the SINR derivation model proposed in [20] in the modeling of a two-tiered macrocell-femtocell environment.

2. Modeling the problem of frequency allocation to a graph theory problem and solving it using a network flow algorithm, that finds the optimal allocation. Optimality is defined against SINR, that is, a solution is said to be optimal if it maximizes the summation of the overall SINR on the currently allocated frequencies.

3. Providing a frequency allocation scheme known for its optimality, and comparing it with other schemes, and presenting recommendations on which schemes

balances the tradeoff between complexity and performance. The proposed scheme can be used in benchmark studies. However, this study is not a benchmark study, rather, it involves the introduction of this scheme.

1.4 Thesis Organization

This thesis is organized as follows. Chapter 2 gives an orientation on indoor coverage techniques that preceded femtocells. Section 2.2 provides the nomenclature and the main feature of femtocell technology, along with its prospective applications. Afterwards, the interference challenge is presented and the current combating techniques are summarized. Chapter 2 also surveys some of the related work in the field of interference mitigation, and provides a comparison.

In chapter 3 the problem in study is mathematically formulated and the proposed solution is presented in detail. Chapter 4 presents the experimental simulation done towards the assessment of the proposed algorithm, along with the achieved results. The chapter wraps up by a complexity and performance analysis that will aid producing recommendations later in this thesis. Finally, chapter 5 concludes and presents future recommendations.

Chapter 2

Background

In this chapter, brief introduction to femtocell technology is presented. An overview for the notions of channel assignment and interference is also offered. The interference challenge and the characteristics of interference in femtocell environments are presented in detail. Afterward, recommendations for interference mitigation solutions are highlighted and some related works from the literature are categorized. Finally, the essence of our proposed algorithm is revealed.

2.1 Indoor Coverage Techniques

Indoor coverage is traditionally achieved via macrocell signalling. Radio planning rules, such as link budget and transmission power, control the level of indoor coverage. Operators try to maintain an acceptable level of 'economic' indoor coverage, that is, satisfying indoor user, hence generating revenue, without much investment in the establishing of macrocells. Nowadays, users expect more reliable and larger capacity communication. Increasing the number of macrocells or transmission power is limited

by budgetary or interference constraints. This is when enhanced indoor coverage becomes a challenge to cellular operators. Due to the importance of indoor coverage and the significant percentage of indoor sessions (data or voice), several techniques have been developed to target this issue [2,9]. This section explains some representative techniques.

2.1.1 Repeaters

Since outdoor signals attenuate heavily at the walls of buildings; an intuitive idea is to have a component that amplifies these raw signals so they can reach indoor User Equipments (UEs) at acceptable power levels. Such a component is called a repeater, and can be one of two types:

Passive repeaters. They amplify signals in a certain frequency band, regardless of their nature. A passive repeater consists of:

1. An external antenna, placed outside a building, pointing to the nearest outdoor antenna sector.
2. An amplifier, to strengthen the signal by amplification, usually leads to a gain of 30-50 dB.
3. An indoor antenna, to redistribute the signal. Directional or omni-directional antennas are typical candidates.

Active repeaters. Are more sophisticated than passive repeaters. They are capable of decoding and reshaping the signal before retransmitting it.

The choice of repeaters is based on the tradeoff between technology and cost. The cheaper passive repeaters can be used in places when the only required enhancement

is signal amplification. While active repeaters can be used in confined areas where much errors are expected, because they can increase the data rate by decreasing the data transmission errors that may occur. On the other hand, passive repeaters are not advised in high error rate environments because when using higher frequencies, the degradation of the signal can greatly affect the quality of the transmission. Proposal that combine both types of repeaters already exist [21].

2.1.2 Distributed Antenna Systems

Distributed Antenna Systems (DAS) [22] are based on the idea of replacing an antenna transmitting at high power with a number of smaller antennas transmitting at lower powers. A number of components can be used to split the signal power between the small antennas. For example, coaxial cables, splitters, taps, attenuators and filters. Like repeaters, DAS can be passive or active. The reader is encouraged to review chapter 2 from [9] for more information about DAS.

2.1.3 Indoor Cells

Prior to the success of WiFi, operators started to consider extending mobile networks via a clever concept; which is having smaller cells that provide good coverage to a specific set of users in an area. This emerged **Picocells**. These new picocells rely on small BSs that use lower power levels and, thus, less capacity compared to the outdoor BSs serving the larger macrocells. A picocell is connected to the core network via standard in-building wiring, fibre optic or Ethernet connections. It connects to an operator Base Station Controller (BSC), which manages the tasks of data transmission between the picocell and the network, performs handover between the cells, and

manages resource allocation to different users.

Femtocells are more different than picocells. More of residential/private/home owned base stations. A femtocell is connected to the operator network directly via the Internet. Femtocells are limited in power and capacity. The classical models of home femtocells demonstrated an output power between 10 to 20 dBm, and supported a number of users between 3 to 5.

2.1.4 Differences Between Femtocells and Picocells

This section provides insight on the differences between femtocells and related technologies. Table 2.1 summarizes the differences between picocells and femtocells. Figure 2.1 shows a comparison between conventional cell sizes.

Criterium	Picocell	Femtocell
Installation	By the operator	By the end user
Connection to the core network	Coaxial or fibre optic	ADSL or cable
Capacity	10-50 users	3-5 users
Coverage	100m-200m	< 50m[1]

[1] For typical home femtocells. Longer range femtocells will be available for larger facilities such as malls and offices.

Table 2.1: Comparison between picocells and femtocells. Reproduced from [9], with modifications.

Picocells rely on the operator network infrastructure. Thus, their positions need to be planned. Femtocells, on the other hand, connect to the core via any Internet connection that allows for the relevant authentication procedures to take place. The operator therefore saves the cost of the additional infrastructure required. They

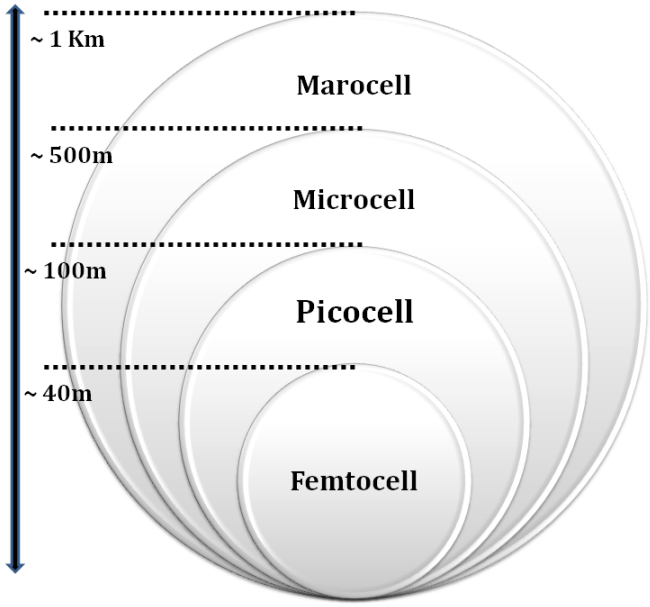

Figure 2.1: Comparison of conventional cell sizes. Reproduced from [9], with modifications.

also have great flexibility in not requiring any planning on part of the operator, or installation costs.

2.2 Femtocells

2.2.1 Nomenclature

This section points out some definitions that will be used throughout this thesis.

FBS. Also known as Femtocell Access Point (FAP), or home base station; a device that resembles regular WiFi access points and is intended to be placed at homes, offices or malls. A FBS is considered the primary communication device in a femtocell network.

Femtocell Networks. Are novel wireless networks aimed at increasing capacity and

coverage of cellular networks indoors. A femtocell network comprises a number of FBSs. They connect UEs to a mobile operator's network via residential Digital Subscriber Line (DSL) or cable. Figure 2.2 is an illustration of a typical femtocell network.

Femtocell. In analogy to a macrocell, a femtocell is the area of coverage of a FBS. It is of importance to point out that the term 'femtocell' has been extensively used in the literature to indicate the physical device itself. Since this is a common mistake, this thesis advocates the use of 'FBS' when referring to the hardware and 'femtocell' when referring to the area of coverage from a networking perspective.

Femtocell User Equipment (FUE). A UE currently associated with a FBS.

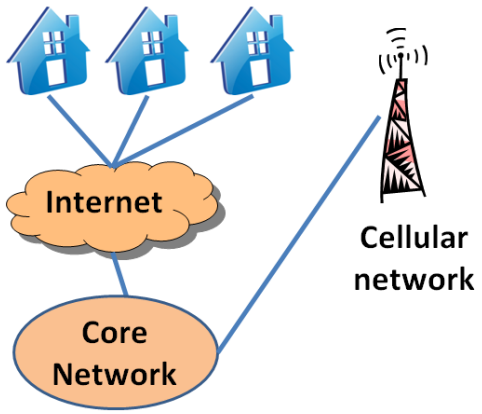

Figure 2.2: Femtocell network connects FBSs to the core network via residential DSL or cable.

2.2.2 Femtocells features and attributes

Some features characterize femtocell technology, among these features [2]:

Usage of mobile technology. Femtocell technology targets complementing the current cellular systems. Hence, it is assumed to integrate with the readily available cellular components including mobile phones and cellular protocols and interfaces. Qualifying standard protocols include GSM, WCDMA, LTE, Mobile WiMAX, CDMA, as well as current and - supposedly - future protocols standardized by 3GPP, 3GPP2 and the IEEE/WiMAX forum.

Operation in licensed spectrum. This allows supporting regular mobile devices without the need of dual-mode devices to use in a femtocell.

Coverage and capacity enhancement. FBSs transmit in relatively very low power targeting a very small indoor area compared to Macrocell Base Stations (MBSs). The very short distance between a transmitter and a receiver promotes the use of higher order modulation schemes and hence promotes higher capacity [22, 23].

Backhauled to the cellular network. Data sent from a FBS is backhauled to the cellular network through DSL or cable, using standard Internet protocols.

Zero-touch feature. FBSs will support plug n' play [24]. This feature mandates that a user should have no involvement in either installing or operating the home device save for powering it on. The initial configuration, re-configuration and the rest of the device operation should be seamless to the user and should not entail any technical support. Although the FBSs will receive their operation parameters via the operator network, this operation will be done automatically under the hood, without any user intervention.

Figure 2.3 shows the main features of a FBS.

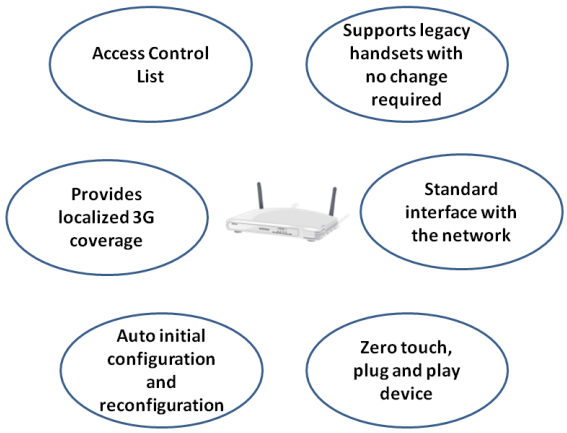

Figure 2.3: Some key FBS features. Reproduced from [9].

Table 2.2 shows a comparison of the general characteristics of femtocells versus other communications devices.

	Wi-Fi Access Points	Cordless Phones	Repeater (Boosters)	Cellular Base Stations	Femtocells
Operates in licensed spectrum	N	N	Y	Y	Y
Supports power control	N	N	Y	Y	Y
Robust Security	N	Y	N/a	Y	Y
Serves existing personal devices	N	N	Y	Y	Y
Provides voice and data services	Y[1]	N	Y	Y	Y
Provides wide-area mobility	N[2]	N	N/a	Y	Y
Consumer installation	Y	Y	N	N	Y

[1] Requires device-specific extension.
[2] Unless combined with mobile systems and special enhancements

Table 2.2: Comparison of femtocells and other wireless devices. [2]

2.2.3 Advantages of femtocells

This section discusses the advantages of femtocells from both the operator perspective and the end user's perspective.

A. Operator Perspective

Any cellular operator is keen to keep its current users satisfied, and races with other competing operators to acquire as many users as it can. Operators try to increase coverage in poorly covered areas and offer value-added services to reduce churn. Churn is the rate of users who stop using a certain service for any reason, and hence stop generating revenue for the operator. Churn has a critical impact on operators within

a competitive environment. This section discusses the benefit of employing femtocells to the operator.

Increase system coverage and capacity. By offloading indoor connections to a femtocell instead of a macrocell. This frees up resources on the macrocell to service more outdoor users. Also, this increases the capacity of indoor users by connecting them to near indoor FBSs.

Filling coverage holes. A MBS adjusts its transmission power to serve as many users as it can. However, the tradeoff between power and interference is resolved by limiting transmission power to a certain level, which results in the creation of 'pockets' or 'holes' between macrocells. Unfortunate users who reside within these holes experience very low signal level, lower than what may be required to make a call. Femtocells fit perfectly in situations like this. Minimal interference from macrocells due to their poor signals will hardly affect the femtocell performance, and at the same time, femtocells will cover a large portion of the gaps.

Reduce churn. Churn represents a considerable loss to operators specially in saturated markets. The value of a current customer increases when less or no other potential customers are out there. Poor indoor coverage can cause churn, however, with the introduction of femtocells, value-added family packages can be delivered to the customer, and hence, reducing churn to a great extent.

Cutting costs. By increasing the system capacity without the need for new cell sites for macrocells, the operator will experience huge savings in terms of CAPEX and OPEX [2, 9, 12, 13, 25].

B. End User's Perspective

Subscribers rush towards better quality services, lower prices, or unique services that are not offered by other operators. While most users are not ready to pay the extra dollar for current services, operators try to convince users with new services in order to increase their revenues. This section presents forms of attraction that femtocells can offer to subscribers.

Better service. In addition to enhanced coverage and capacity stated before, femtocells will also help the operator provide richer services like femtozone-based services, and bundled services, and other bandwidth consuming applications, which will also encourage mobile usage indoors [25].

Cheaper prices. By installing new base stations inside homes, that will also be maintained later by the end user; operators can offer value-added services like free or cheap calls from home or free 'inside-office' calls.

Centralized management. Femtocells can offer a single address book and one billing account for both land line phone, broadband and mobile phone.

Saving power. Because of the short distance between a FBS and a UE; battery operated devices will communicate using lower power levels than those required to communicate to a macrocell, resulting in longer battery life. This will also reduce health concerns on using mobile devices.

Femtocell nature will attract consumers for a number of reasons. For instance, femtocells will not require users to have dual-mode devices which will relief the worry of purchasing new devices that are compatible with femtocells. Also, the fact that

femtocells will be available in Closed Subscriber Group (CSG) mode gives consumers a sense of security and privacy.

2.2.4 Some femtocell applications [9]

Femtozone services. Services based on the presence of mobile devices within the coverage area of a home femtocell. For example, the FBS can send an SMS when a user enters the femtozone, or synchronize pictures and videos from a trip [25]. Another promising application can be a 'virtual number' to reach all people currently in the house, or for holding conference calls with family members. Enterprise VoIP [26], and file transfer [27] can also be categorized as femtozone services.

Connected home services. Home automation applications and controlling home equipments via mobile phones are good examples of connected home services that are expected to spread with the introduction of femtocells.

2.3 Channel Assignment

Channel assignment is the process of assigning bandwidth to BSs to be split later among UEs. Bandwidth is needed to transmit signals modulated with data. Channel assignment, frequency allocation, frequency scheduling; these definitions have been used interchangeably in the literature to indicate the process of assigning frequency slots to terminals to transmit data over them. The quality of an assignment is governed by many factors:

Complexity. Less complex frequency allocation is more favored than complicated procedures. In advanced network architectures, the rate by which the frequency

allocation can occur is as high as once every 10ms.

Bandwidth fragments. Some channel allocation schemes uses fixed allocations, which may cause bandwidth fragments, and decrease the utilization of bandwidth.

SINR. Is a measure of how good a link between a BS and a UE. Changing the allocated channel(s) affects the resulting SINR.

In short three types of channel allocation strategy exist [28]:

Fixed Channel Assignment (FCA). Is a technique where a pre-computed fixed set of channels is assigned to a cell. The channel sets are computed to be less vulnerable to Co-Channel Interference (CCI). However, this scheme might cause sessions in crowded cells to be rejected when resource admission cannot be granted.

Dynamic Channel Allocation (DCA). Is a technique where channels are allocated 'on-demand' as cells request them for transmission. This technique is considered more resource-aware but renders the system more interference vulnerable. Thus, requires more calculations and real-time data on channel occupancy, traffic distribution and Received Signal Strength Indicator (RSSI).

Hybrid Channel Allocation (HCA). Uses both FCA and DCA in conjunction. The process involves FCA for some resources then DCA for the rest. As per [28] This technique has been adopted by some fairly old studies like [29–31]. It can also been seen from the modern literature that studies concerned with HCA are still on track [32].

2.4 Interference Challenge

Generally, interference occurs when two or more devices are transmitting 'near' each other. The definition involves devices that are either physically near each other, or devices transmitting on near frequencies or channels. As is well known, the wireless medium faces many types of interference. For example, Inter-Symbol Interference (ISI), which occurs when a symbol overlaps with following symbols due to the delayed multi-path signal. Co-Channel Interference (CCI) occurs when a device transmits on the same channel being used by a nearby device. Whereas Adjacent Channel Interference (ACI) happens when signals from a device transmitting on a certain channel interfere with signals of another device on another channel.

FBSs are meant to be installed indoors to cover relatively very small areas compared to traditional macrocells. Unless deployed in very remote areas, femtocells will always be overlaid on macrocells, rendering such deployments as a two-tiered, composed of a macro-tier and a femto-tier. This tiered deployment is vulnerable to cross-layer interference [9, 10, 17], which is the type of interference that occurs between cells of different types, e.g., Femto-to-Macro or Macro-to-Femto. In addition to cross-layer interference, co-layer interference might occur between two cells within the same layer See Figure 2.4 for a simple illustration of interference types in a femtocell environment.

2.4.1 Mitigating Different Interference Types

Cross-layer interference can be greatly reduced by a setup through which the available spectrum is partitioned between the macrocellular and the femtocellular layers. This setup, however, limits the amount of spectrum available for each layer and is considered

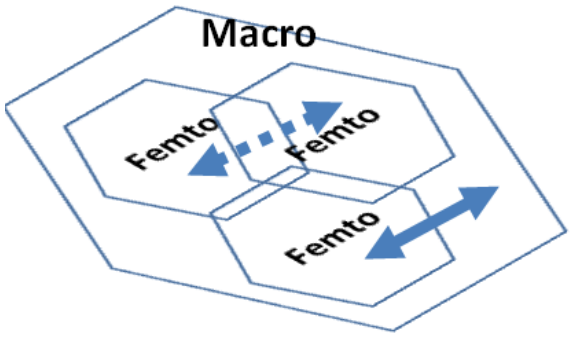

Figure 2.4: Interference types in a femtocell environment: the dashed line shows co-layer interference and the solid line shows cross layer interference

less efficient [6]. On the other hand the whole spectrum or part of it can be shared between the two layers resulting in larger system capacity, but rendering the system more interference vulnerable. In [33] the authors proposed a hybrid spectrum sharing technique, trying to achieve a lower interference and a high capacity system at the same time. Conversely, co-layer interference can be mitigated to a great extent using proper frequency allocation and scheduling techniques, or dynamic power adjustment.

In this chapter, representatives of the different techniques that have been devised to mitigate different interference types will be discussed. Section 2.6 presents the result of a literature survey that was conducted for this purpose.

2.5 Interference Mitigation Solutions

Innovative interference mitigation techniques should be used with this novel type of sophisticated networks. Proposals to mitigate interference should take into consideration the nature of femtocells for a number of reasons:

1. Femtocells operate in licensed spectrum.

2. FBSs are installed and maintained by end users.

3. FBSs have limited computation and signalling power compared to regular outdoor BSs.

4. Femtocells are in most cases overlaid on macrocells

Using these facts, we can derive a number of parameters that should be considered when designing femtocell interference mitigation solutions to ensure applicability:

Complexity requirements. Unlike the regular MBSs, the initial objective of a FBS is to provide better indoor voice and data services in a simple and cost effective way. This results in a small size FBS with limited computation and processing power. However, deployment issues necessitate avoiding complex algorithms for the mitigation purposes. By surveying the literature, we speculate that optimized algorithms based on Computational Intelligence (CI) like Genetic Algorithms (GAs), Simulated Annealing (SA), Neural Networks (NNs) and Game Theoritic-based algorithms will gain momentum in the context of research to provide stronger solutions.

Distributed Operation. In order to minimize decision delay, it is important that localized decisions are made, foregoing centralized processing, and the delays required for the two-way signalling.

Adaptability. Distributivity is often linked to adaptability. Interference mitigation algorithms are expected to be highly adaptable to the surrounding environment since new FBSs can be deployed anywhere at anytime which will keep the current network infrastructure topology in a state of continuous change compared to the ordinary cellular network.

Scalability. The projected density of deployment for femtocells also necessitates scalable solutions. To appreciate the minimal scale of deployment, the installation of a FBS per household should be assumed. This projected enormous volume entails highly scalable solutions.

One important aspect that should be also regarded is self-organization [34, 35]. The aforementioned zero-touch feature [24] mandates that a FBS be able to do self-configuration, self-optimization, and self-healing [9, 18]. The self-configuration characteristic mandates that a device, once powered up, starts collecting its configuration parameter and does configuration tasks, whether these parameters are hard-coded, on-chip, or reside on some server. On the other hand, self-optimization ensures that the device is always in a state of optimizing parameters such as signalling, power and frequency allocation to guarantee calm and effective communication. Finally, self-healing states that if certain communication failure or degrading happens, the device should find fixes and apply them to continue operation. Self-organization is composed of all three, and is needed to ensure that the FBS unit can function on its own. Self-organization has been proposed at different phases of femtocell standardization. It can also be linked to adaptability because a FBS is in a continuous state of operation optimization. Signalling, power level and computations are examples of what can be optimized whilst the operation of a FBS.

2.5.1 Solutions Categorization

Interference mitigation solutions can be categorized against a number of criteria:

Operator managed vs FBS vendor managed. An operator managed solution affirms that the cellular provider coordinates the work of different femtocells and

supplies them with parameters for operating interference mitigation solutions; whereas a FBS vendor managed (on-chip) solution requires that FBSs ship pre-configured with certain interference mitigation out-of-the-box mechanisms regardless of the network they will be deployed as part of.

Locality. A localized solution runs at each femtocell, without the need for central coordination of calculations between FBSs. Localized techniques are more preferable to support scalability which requires that a FBS works on its own or in rare cases communicates with the surrounding FBSs. Conversely, network-wide techniques provide acceptable operation with generally less sophistication because they depend on specific central entities that aggregate information from groups of femtocells and use this information to compute solutions. Local versus network-wide solutions are also referred to as decentralized versus centralized solutions.

Application level. Categorization per application level describes the level of granularity at which the solution is applied, i.e., at the tier level or at the cell level. Solutions deployed at the coarse grained tier level tend to use durable, less or no changing parameters. In contrast, fine grained cell level solutions work on a much lower level and they need to be more adaptable and highly configurable. An example to show the difference between tier level and cell level is frequency planning in opposition to frequency allocation. In a multi-tier environment portions of the spectrum is split among tiers, without going deeper to cells; this is a tier-level technique. On the other hand, frequency allocation, where users within a cell are admitted frequency slots for transmission, is considered a cell-level technique.

2.6 Related Work

2.6.1 Current Techniques

Recently, many studies have been proposing interference mitigation techniques according to different environment setups and different scenarios. The resulting solutions range from basic optimizations to sophisticated powerful solutions. The latter ones are less dependent on physical and Medium Access Control (MAC) layers and are more efficient in terms of signalling, but at the cost of intensive computations. In what follows, we summarize these different techniques.

Frequency planning. Interference can be mitigated at the planning stage as it is possible, for example, to split the available spectrum into bands among cells within a cellular system to minimize intercell interference, i.e., interference that occurs within adjacent cells when UEs on the edge of cells receive mixed signals.

Spectrum splitting. In multi-tier networks, operators use spectrum splitting to dedicate portions of the spectrum to different tiers. Some solutions support high level of sharing between tiers, resulting in a higher capacity but more interference vulnerable systems. Meanwhile, other solutions can be based on total spectrum separation between layers which provide greater resistance to interference but at the cost of lowering the system capacity. Hybrid systems were also proposed, e.g. in [33], to define a solution based on the trade-off between interference and capacity. Spectrum splitting is used mainly to combat cross-layer interference.

Power control. Is a solution applied at the cell level. It aims at adjusting the transmission power of BSs to limit unnecessary high power that might cause interference with the surrounding cells, or affect near transmissions.

Frequency allocation. Is another cell level solution aiming at combating interference by proper allocation of frequency channels to users. Subcarrier allocation, which has been recently adopted with new access technologies, such as OFDMA, has been studied thoroughly as an effective way of combating interference. Fractional Frequency Reuse (FFR) [36, 37], Dynamic FFR [38], and Dynamic Frequency Selection (DFS) algorithms [39] have been proposed in this matter.

More recently, different studies have addressed interference mitigation. The following paragraphs shed the light on candidate interference mitigation solutions to familiarize the reader with the state of the art related studies from the literature.

In [40], the authors advocate the importance of distributed, self-optimizing schemes due to the fact that locations and the number of FBSs exploit a high level of uncertainty. The authors solve an optimization problem to control the overall transmission power of FBSs in a femtocell OFDMA network, subject to individual rate and power constraints. According to the authors, an optimal solution requires information about all communication links, and this kind of information is not readily available at all times. So, the authors propose a distributed power control and scheduling algorithm as explained in the next paragraph.

Each user has a Quality of Service (QoS) constraint in the form of a threshold SINR for a given service; the objective is to meet the required SINR at each user. The problem is modeled as a Linear Programming (LP) problem and is solved using Particle Swarm Optimization, an example of a Swarm Intelligence (SI) approach. SI exhibits the communal behavior of self-organizing entities in a distributed environment. Many of the techniques categorized as SI approaches are copied from nature, such as ant colonies and animal herding. The proposed algorithm yields sub-optimal solutions

on each femtocell and in the event that no feasible solution exists, a heuristic sacrificial mechanism is employed to defer some transmissions of users causing high interference based on the users' nominal SINR. The algorithm is based on heuristics and takes into account the femtocellular layer only and involves alot of signalling, but in favor of being decentralized.

In [28], the authors suggest two reuse partitioning schemes to be applied on overlaid - multiple layered - networks. The main idea involves adapting cluster size to maintain high Signal to Interference Ratio (SIR), and applying channel assignment. Each hexagonal cell can be viewed as a set of concentric hexagonal cells, each with a different radius.

Two schemes were proposed: 1. Maximal Dynamic Reuse Partitioning (MDRP), and 2. Optimal Dynamic Reuse Partitioning (ODRP). In MDRP, excess channels are assigned to the innermost region in order to acquire maximum effective capacity from the subject cell. Alternatively, in ODRP, the system allocates unused channels in line with the areas and the distribution of users within the concentric SIR regions, in order to maintain a certain Grade of Service (GoS). The adaptive nature of the proposed schemes makes them more powerful than similar schemes.

In [41], the authors study mitigating downlink Femto-to-Macro interference through dynamic resource partitioning. The system under study is an OFDMA two tiered network that employs universal frequency reuse. Since the transmission power of eNode Bs (eNBs) is much more than that of Home eNode Bs (HeNBs), then it is likely that Macrocell User Equipments (MUEs) within the transmission range of femtocells will cause interference to the UEs around, and will itself experience low SINR. To preserve universal frequency reuse, the authors suggested prohibiting HeNBs from

accessing downlink resources that are assigned to near MUEs. By doing so, interference to the most vulnerable MUEs - as per the authors - is effectively controlled at the cost of sacrificing minor portion of the femtocell capacity. The study is based on the assumption that giving up some femtocell resources will lead to a better system throughput. The authors defended this assumption in their study.

In [42], the authors propose a greedy based dynamic frequency assignment scheme. The core idea of the scheme is to assign the quietest channels to femtocells according to the received power level. The algorithm is two-fold: 1. Each FBS scans the entire spectrum and selects the frequency bandwidth that shows the lowest received power level, and 2. Each FBS measures then sorts the received power level on every sub-channel of its frequency bandwidth and assigns the quietest sub-channels to its UEs. The algorithm may not yield powerful results compared to similar algorithms in the field, but is considered fast and not complex, especially that it works in a decentralized manner.

In [43], the authors exploit coverage adaptation through balancing FBSs transmission powers. Power control decisions are made according to the available mobility information about the surrounding users. And the goal is not to leak much pilot signal outside a house, which may lead to increasing mobility events, or decrease the power too much, which may also cause the same problem. The study is considered a contribution to the auto-configuration and self-optimization aspects in femtocell networks. The paper distinguishes between auto-configuration and self-optimization in the sense that auto-configuration is responsible for initially configuring the FBS, whereas the self-optimization is concerned with enhancing the current configuration during operation.

Auto power configuration is proposed via three different approaches:

Fixed power. All FBSs start transmission with a fixed power. This is considered the easiest approach of all, but clearly it can be enhanced with simple calculations as depicted in the two other approaches.

Distance based. A FBS starts transmission with a power value such that the surrounding UEs receive this power as strong as the power received from the macrocell. This way, unnecessary mobility events can avoided to a great extent. The macrocell power is estimated using a path-loss model.

Measurement based. Works as distance based, but the difference is that the macrocell power is not estimated, rather is measured by the FBS. This requires a built-in measuring capability in the FBS.

After auto-configuration, self-optimization comes into play. The proposed self-optimization approaches aim at minimizing the number of mobility events.

In [32], the authors assume a two-tier (femto-macro) environment, and present the capacity-interference tradeoff resulting from using shared bandwidth versus using dedicated bandwidth. The proposed idea is splitting the area around a macrocell into inner and outer regions. A FBS within the inner region will not operate in a co-channel mode (shared bandwidth) to avoid interference, rather it uses a frequency band other than that used by the MBS. The authors tackled the calculation of the best threshold the splits the inner and outer regions. Interference Limited Coverage Area (ILCA) is derived via estimating power levels using different path-loss models.

In [44], the authors study the effects of two power control schemes namely geo-static power control and adaptive power control. In geo-static power control, the

transmission power of a femtocell is based on its distance from the macrocell. However, in adaptive power control, the transmission powers of femtocells are adjusted based on the network target rates, enhancing the femtocell users' throughput without much degradation in the macrocell performance.

In [45], the authors use a non-cooperative game theoretic approach to model the distributed power control of femtocells, where each FBS is a player trying to decide its transmission power whilst maximizing its benefit. The system considers fairness in its model too; femtocells serving more mobile stations should be allowed to transmit at higher power levels to maintain service to its users. A payoff function based on revenue and cost was derived, where the cost is directly proportion to the transmission power, to advise FBSs to reduce their transmission powers. Transmission powers reach Nash Equilibrium (steady state) in the simulated game. Game theory has been also used in other femtocell interference mitigation related studies [46, 47].

In [12], the authors study a centralized Radio Resource Management (RRM) for femtocell dense deployment. They derive an objective function to maximize the system capacity. The problem is divided to two sub-problems: 1. sub-channel allocation, and 2. Power allocation. In [48] the authors advocate the idea of preventing some frequencies from being used by a femtocell if they are already assigned to a near MUE. Availability of macrocell frequency scheduling information is assumed.

2.6.2 Discussion and Motivation

We studied the recommended characteristics of future interference mitigation solutions. Based on the comparison from the literature presented in this thesis, we can infer that there is still a large void when it comes to optimized solutions. We have been

studying the applicability of a centralized frequency allocation algorithm, that makes use of graph theory and optimization. The addition to what is currently offered in the literature is seeding the optimization. We focus on using optimal assignment algorithms rather than random or greedy based assignments. This should boost the performance of our technique when we devise a decentralized version of it. We take into consideration the fact that femtocells are overlaid on macrocells, so we incorporate both layers in the algorithm dynamics. We also take into account the trade-off between complexity and performance, to produce a high quality applicable solution that we believe it will assist in filling the gap in the current interference mitigation solutions.

Table 2.3 shows a comparison between recent studies from the literature. Last entry in this table is our proposed solution.

In the next chapter, we are proposing a novel approach that models the spectrum allocation problem as an assignment problem, and solves it using a graph theoretic approach in an efficient and optimal way. The solution is based on a popular network flow solution, namely the Minimum Cost Flow (MCF) algorithm. A resulting assignment is considered optimal if the summation of SINRs of the assigned RBs is maximized. The proposed solution runs in a centralized manner, so it is assumed that there will be a central entity to gather information from BSs and manage the algorithm running to find the best possible frequency assignment to all users within a macrocell and the overlaid femtocells.

Study	Direction	Locality	Technique	Optimization Method
Akbudak et al. [40]	Downlink	Decentralized	Power control, frequency scheduling	Particle Swarm Optimization and heuristics
Aki et al. [28]	N/a	Decentralized	Channel allocation	N/a
Bharucha et al. [41]	Downlink	Decentralized	Spectrum partitioning	N/a
Zhioua et al. [42]	Downlink	Decentralized	Frequency planning, Frequency assignment	Greedy-based
Claussen et al. [43]	N/a	Decentralized	Power control	Feedback-based iterative optimization
Guvenc et al. [32]	Downlink	Centralized	Frequency planning	N/a
Arulselvan et al. [44]	N/a	Decentralized	Power control	Feedback-based iterative optimization
Hong et al. [45]	N/a	Decentralized	Power control	Game theory
Kim et al. [12]	Downlink	Centralized	Sub-channel allocation	Iterative optimization
Proposed approach	Downlink	Centralized	Frequency allocation	Graph theory, Network flow

Table 2.3: Comparison of recent interference mitigation studies.

Chapter 3

Problem Formalization and Proposed Solution

This chapter describes the problem context in detail, in terms of technologies and infrastructure assumed. It also discusses how resources are requested and assigned. Moreover, it describes the nature of the problem in study, modeling it to an assignment problem, and solving it using graph theory. The proposed solution reduces the assignment problem to a network flow problem, and solves it using MCF algorithm.

3.1 System Description and Problem Definition

3.1.1 System Description

This study is concerned with downlink interference mitigation by proper frequency allocation in OFDMA networks. Mixed OFDMA networks comprising femto-tiers layering macro-tiers are considered. The preceding statements can be broken down into a set of characteristics that describes the environment upon which the proposed

scheme should be run:

OFDMA System. As the air interface technology of choice for downlink in LTE, OFDMA is considered in simulation.

Downlink. The study focuses on downlink direction instead of both, downlink and uplink directions. Specialty in this matter allowed for the development of a tailored powerful algorithm.

Tiered Deployment Model. Practicality mandates that the proposed algorithm supports tiered deployment, where femtocells layer macrocells. Simulating such deployment as it seems a bit harder, is closer to the reality, and this will create a more practical scheme than many other schemes in this area.

High Level Operation

In an OFDMA system with mixed BSs - (FBSs and MBSs) - one possible spectrum management scheme is using shared spectrum, instead of dedicated spectrum, also known as co-channel operation, where the bandwidth is shared between the macrocellular and the femtocellular layers. Each BS has a finite number of Resource Blocks (RBs) representing the available spectrum, and has a number of UEs uniformly distributed within the cell radius. At each BS, downlink SINR is calculated as presented in [20]. For each femtocell, a matrix is created, composed as the arrangement of the calculated SINR values, where a row represents SINR values for a specific UE per each RB. A centralized entity aggregates all matrices generated at all BSs to compose one matrix of all UEs against RBs. MCF algorithm is then run on this matrix to produce an optimal solution in terms of maximizing the total SINR.

3.1.2 Problem Definition

Consider the aforementioned OFDMA network with two layers, a femtocellular layer within a macrocellular layer. The macrocellular layer is the traditional layer in the cellular network which encompasses MBSs deployed at specific cell sites, whereas the femtocellular layer consists of several shorter range cells resulting from the deployment of FBSs in an ad-hoc manner. Each BS has a number of UEs to serve. UEs that belong to the femtocellular layer, i.e., connected to FBSs, are referred to as Femtocell User Equipments (FUEs), whereas UEs connected to a MBS are referred to as Macrocell User Equipments (MUEs). UEs are served in units of RBs. In OFDMA downlink, a RB is a basic time-frequency unit (see Figure 3.1), it consists of 12 consecutive subcarriers in the frequency domain and 7 OFDM symbols in the time domain, assuming normal cyclic prefix.

The minimum unit to serve a UE is a RB, that is, a user is either admitted access to a whole RB or not. The problem investigated in this study is the assignment of resource blocks among system users. An optimal assignment algorithm is proposed, aimed at maximizing the system capacity.

3.2 Mathematical Formulation

Given L mixed - femto and macro - BSs labeled 1 through L, let U_j be the number of UEs associated with BS j, where $1 \leq j \leq L$. For each cell one can measure the SINR for each UE per each RB. This can be arranged in a matrix $S_{U_j,R}$ where R is the number of RBs in the accessible spectrum. Each entry in this matrix signifies the SINR that a UE will experience when assigned a specific RB.

All resulting SINR matrices of all BSs are aggregated into one matrix $\Gamma_{U,R}$ by

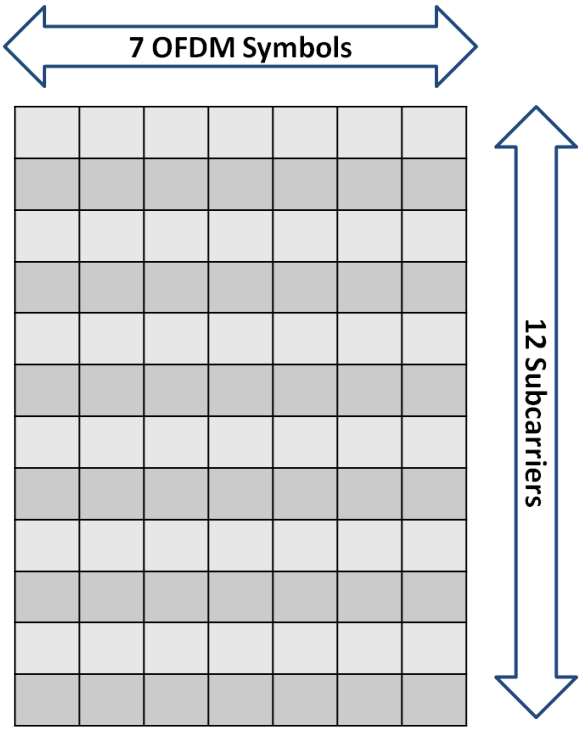

Figure 3.1: Normal Cyclic prefix OFDMA downlink Resource Block

adding the rows representing the UEs into the matrix. Let $\gamma_{u,r}$ be an entry in Γ, it represents the SINR that a UE denoted by u, $(1 \leq u \leq U)$, will experience if assigned a RB denoted by r, $(1 \leq r \leq R)$.

Let $\omega_{u,r}$ be a binary output function indicating whether a RB r is assigned to a UE u or not, such that $\omega_{u,r} = 1$ if RB r is assigned to UE u, and 0 otherwise.

The proposed algorithm maximizes the summation of the chosen SINR values.

In mathematical terms we are trying to maximize:

$$\sum_{u=1}^{U} \sum_{r=1}^{R} \omega_{u,r} . \gamma_{u,r} \tag{3.1}$$

Subject to constraint:

$$\sum_{\forall u} \omega_{u,r} \in \{0, 1\} \tag{3.2}$$

The objective function in expression 3.1 indicates that the summation of SINR of all assigned RBs is to be maximized, while the only constraint in expression 3.2 means that a RB will be assigned to at most one UE.

3.3 Problem Categorization and Proposed Solution

3.3.1 Problem Categorization

The problem falls under the category of Assignment Problems. In general, assignment is a combinatorial optimization, that involves assigning or 'matching' elements to other elements in a manner that a satisfies a set of criteria. Any assignment problem can be visualized as a graph $G(N, E)$, where N is a list of nodes - or vertices - and E is a list of edges that connects between graph vertices.

The specific problem of assigning RBs to UEs can be modeled as a Transportation Problem [49]. In a Transportation Problem a set of graph nodes N is partitioned into two subsets U and V (not necessarily of equal cardinality) such that:

1. Each node in U is a supply node.
2. Each node in V is a demand node.
3. A set of edges running between the two subsets exist. Each edge (i, j) joins a node $i \in U$ with a node $j \in V$

The classical example of this problem is the distribution of goods from warehouses to customers. In this example, warehouses are represented by nodes in U and customer

zones are represented by nodes in V. An edge (i, j) represents a distribution channel from warehouse i to customer j. Usually a cost function is associated with each edge to indicate the incurred cost of using this edge in a solution.

Note that since the two subsets U and V are disjoint. Accordingly, the ordering of sets does not matter, and edges that run between subsets can still be modeled as directed edges. To make the implementation easier, the proposed solution uses this kind of modeling variation, so it is worth mentioning here. In the proposed solution U represents the demand nodes and V represents the supply nodes, a link (i, j) means a node i is supplied via node j.

The generic modeling of this problem is a bipartite graph (see figure 3.2), with two disjoint sets U and V.

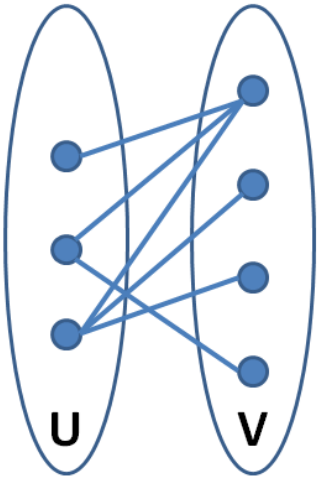

Figure 3.2: Example of a bipartite graph.

3.3.2 Proposed Solution

MCF is known to give the optimal solution to a network visualized as a directed weighted graph, and this optimal solution represents a set of edges chosen such that

$$\begin{matrix} \gamma_{1,1} & \gamma_{1,2} & \cdots & \cdots & \gamma_{1,R} \\ \gamma_{2,1} & \gamma_{2,2} & & & \gamma_{2,R} \\ \vdots & & \ddots & & \vdots \\ \vdots & & & \ddots & \vdots \\ \gamma_{U,1} & \gamma_{U,2} & \cdots & \cdots & \gamma_{U,R} \end{matrix}$$

Figure 3.3: Example of SINR matrix.

the summation of their weights/costs is minimized [50]:176. Assuming that we have the global SINR matrix Γ as described before; it can be visualized as a directed graph with two disjoint sets of nodes representing UEs and RBs, U and V respectively. Graph edges originate from nodes in U to nodes in V, and the cost of a link between node $i \in U$ and node $j \in V$ equals $\gamma_{u,r}$.

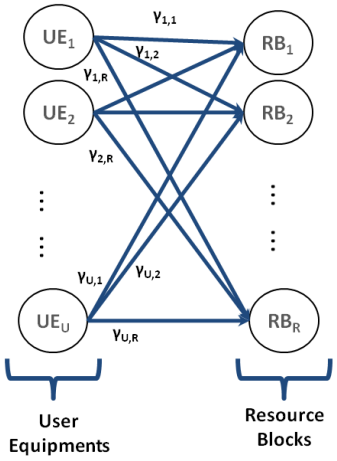

Figure 3.4: Mapping SINR matrix to a Bipartite graph.

It can be seen how the matrix in Figure 3.3 can be mapped to the directed graph as in Figure 3.4, this technique has been used to supply MCF with a graph to work on. Since a typical MCF problem calculates the flow between a single source and a sink; an artificial source preceding all nodes in U and an artificial sink following all nodes in V were added (See Figure 3.5). Links from/to the artificial source/sink are of zero

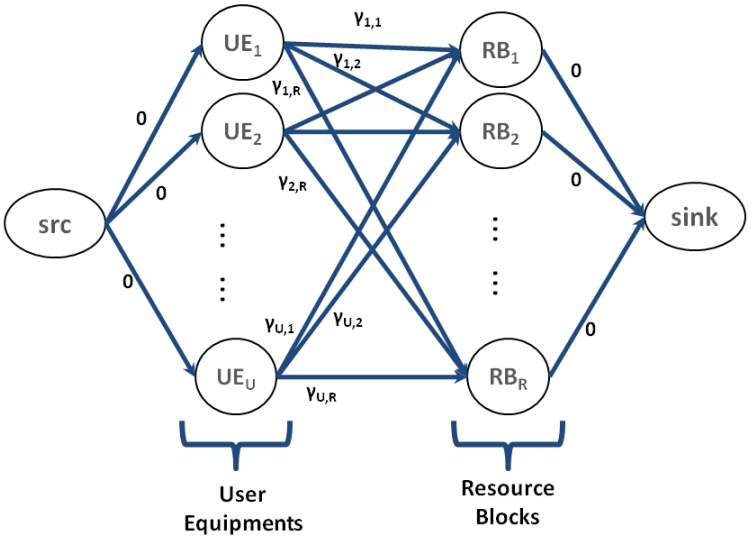

Figure 3.5: Bipartite graph after adding artificial source and sink.

cost, in order not to affect the calculations. For each BS the SINR values for all its UEs against all available RBs are evaluated. All the resulting matrices are aggregated into one matrix of all UEs per each RB. The matrix is then converted to a directed graph and solved via MCF. After running the algorithm, the resulting assignment will highlight edges that give the maximum summation of the SINR values on these edges, and hence this assignment can be considered as one of the possible optimal assignments.

Numerical Example

This is a crude example of the original assignment problem. Assume there is a set with 3 nodes $\{A, B, C\}$, and another set with 7 nodes $\{1, 2, 3, 4, 5, 6, 7\}$. The goal is to assign exactly two nodes from the second set to one node from the first set such

the total summation of the assigned values is minimized.

Assume the costs of assigning a node from the second set to a node from the first set are described in an adjacency matrix, as in figure 3.6.

	1	2	3	4	5	6	7
A	0.378	0.245	0.174	0.379	0.839	0.632	0.000
B	0.341	0.971	0.293	0.560	0.717	0.197	0.023
C	0.481	0.432	0.766	0.799	0.821	0.440	0.110

Figure 3.6: A graph represented as an adjacency matrix.

Figure 3.7 shows how the optimal solution should look like. The adjacency matrix described above is repeated, and the bold, underlined values indicate the values that have been chosen for the optimal assignment. For example, nodes 3 and 4 are assigned to node A.

	1	2	3	4	5	6	7
A	0.378	0.245	**0.174**	**0.379**	0.839	0.632	0.000
B	**0.341**	0.971	0.293	0.560	0.717	**0.197**	0.023
C	0.481	**0.432**	0.766	0.799	0.821	0.440	**0.110**

Figure 3.7: A solved adjacency matrix showing the chosen values minimizing the overall summation

Notes

- The algorithm is not a greedy-based algorithm (for example, the least two interference values in the given matrix, 0.0000 and 0.023, were not chosen in the optimal solution). From another alternate view, the least interference value for row B (0.0232) was not chosen, and the least interference value for column 7 (0.000) was not chosen as well. Choosing any of these will lead to a higher final cost.

- The resulting summation (1.633) is the *absolute lowest value* of all solutions that can be achieved given the problem constraints (2 nodes from the second set should be associated to a node from the first set), that is, the algorithm is designed to find the optimal solution.

3.3.3 Minimum Cost Flow

Description of a Flow Problem

A flow problem can be visualized as a set of connected pipes with different sizes (referred to as: capacities, which is the maximum number of flow units that can flow through a pipe), and the goal of the problem is to find a maximum flow of water for instance, from the start/source of this network to the end/sink of it. This maximum flow is bounded by the capacities of pipes; within each different path from source to sink, the maximum flow in a path will be capped by the minimum flow among all tubes on this path.

A MCF problem adds a new constraint to the original problem other than the pipes capacities, namely the cost. The flow of water in a pipe is subject to a certain cost that is predefined to this pipe. So while maximizing the anticipated flow through the network, the cost of this flow is minimized, and this is why the problem is sometimes called: Minimum Cost Maximum Flow.

What is a Maximum Flow?

A final maximum flow always satisfy the following:

- The total flow through the network is summation of the assigned flows on the edges leaving the source, or alternatively entering the sink.

- A flow on an edge is always less than or equal to the capacity of this edge.
- The sum of aggregated flows leaving a vertex equals to the sum of aggregated flows entering it.
- This sum is maximal.

In addition to a maximum flow solution, a minimum cost solution satisfies that this maximum flow considers the minimum cost applicable.

Graph Representation in a MCF Problem

This section is essential if the reader is planning to read Example 3.3.3.

Vertex. Is a node in the graph where:

- vertex.distance is the shortest distance so far from the source node to the current node (in terms of cost). In other words, it keeps track of the minimum cost incurred to reach this vertex from the source.
- vertex.flow is the amount of units flowing through this node.
- vertex.parent is the immediate predecessor of this node.

Edge. Is a directed link between two nodes/vertices where:

- edge.start: is the node where this link originates from.
- edge.end: is the node where this link is directed to.
- edge.capacity is the number of flow units that can flow through this edge.
- edge.cost is the distance traveled through this edge from start to end.

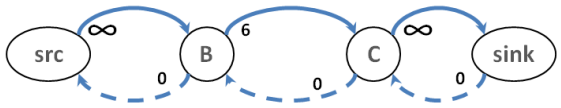

Figure 3.8: Different data structures in a MCF problem

Reverse Edge. An artificial opposite (dual) edge to every directed edge, with negative cost and - initially - 0 capacity.

The role of a reverse edge is to keep track of how many flow units are currently flowing in the corresponding edge and - possibly - roll back a flow in favor of a more preferable flow, Example 3.3.3 shows the usage of reverse edges in detail.

Residual Network. Is the state of the original graph at any point through the algorithm life time. Costs and current capacities of edges can be inferred from the residual network. See Example 3.3.3.

In figure 3.8 Two vertices - B and C - exist, in addition to a source and a sink. There's an edge between B and C where edge.start = B and edge.end = C, edge.capacity = 6. A reverse edge with 0 capacity exist, which means that nothing is flowing from B to C yet. This is explained further in 3.3.3

Dynamics of a MCF algorithm

The algorithm runs in one loop, in each iteration:

- A call to a shortest path algorithm takes place, finding the shortest path from the source to the sink.
- This path is 'augmented' to the current solution, i.e. the flows on the links along

this path are subtracted from the capacities on these links, and added to the capacities of the reverse edges.

Remember that each edge has a negative cost of the reverse edge, this allows us to 'rollback' or trade some of the assigned flows, the following example illustrates it all.

Example

This is a generic Maximum Flow example, where given a network of pipes, capacities available on these pipes, and costs of using a pipe, it is required to maximize the flow from source node to sink node maintaining the minimum cost possible.

Figure 3.9 shows the initial graph. The numbers on the edges indicate the amount of flow available on this edge. For simplicity, costs on all edges are assumed to be 1 which makes the cost of a path between any two nodes equals to the number of hops between them. The source is labeled X and the sink is labeled Y. Figure 3.10(a) shows the residual network for this graph along with reverse edges. Reverse edges start with a zero flow. The algorithm runs as follows:

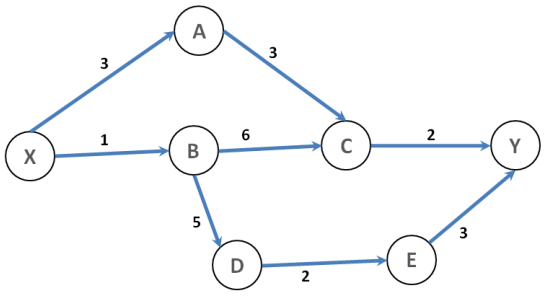

Figure 3.9: The initial network graph with available flows indicated on the arrows.

1. A shortest path call from X to Y is invoked, which - based on the number of

hops - should yield to either $X - A - C - Y$ or $X - B - C - Y$. Assuming the latter was chosen, all edges along this path will have their flows decreased by the minimum flow observed on this path which is 1, whereas reverse edges will have their flows increased by 1. As a result of this step the flow between X and B will be 0 and hence $X - B$ will not be considered when qualifying another shortest path between X and Y. Figure 3.10(b) show the residual network after this step.

2. The next call to a shortest path yields $X - A - C - Y$, decreasing all flows along this path by 2 and adding 2 to the corresponding reverse edges, Figure 3.10(c) show the residual network after this step.

3. One more call to a shortest path yields $X - A - C - B - D - E - Y$, with an extra flow of 1. Note that since there was a flow from C to B it was considered when calculating the shortest path. Having $C - B$ in the shortest path means that the 1 flow unit that was flowing through $B - C$ to reach Y before will flow in the path $B - D - E - Y$ instead, also one of the flow units that were flowing in $C - Y$ will instead come from the path $X - A - C$.

4. A subsequent call to a shortest path from X to Y will yield no more paths. The final residual network is shown in figure 3.10(d) and the final flow network is shown in figure 3.11.

Below is a pseudo-code for the max flow algorithm that solves an assignment problem.

Pseudo-code

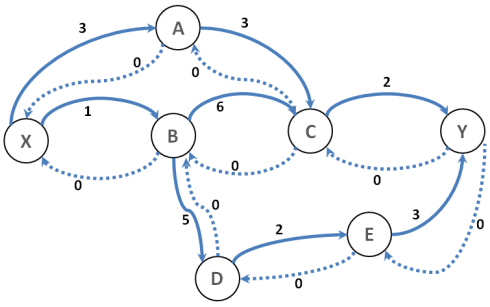

(a) Residual network for the initial graph

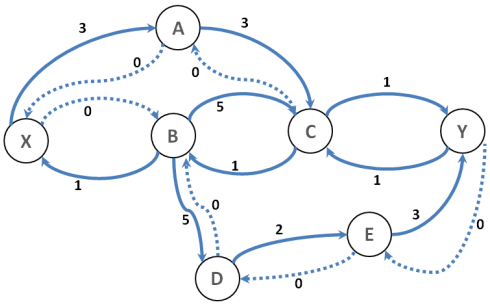

(b) Residual network after shortest path: $X - A - C - Y$

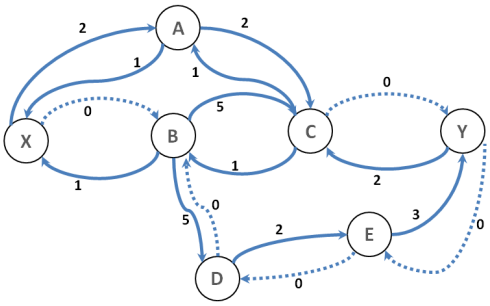

(c) Residual network after shortest path: $X - B - C - Y$

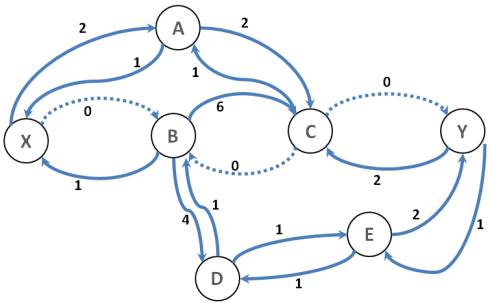

(d) Residual network after shortest path: $X - A - C - B - D - E - Y$

Figure 3.10: Residual network evolution through the algorithm life time.

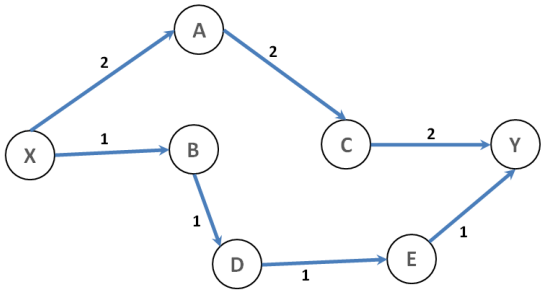

Figure 3.11: The final maximum flow network.

Algorithm 1 BellmanFord shortest path algorithm.
Function BellmanFord(list vertices, list edges, vertex src)

```
1: for all vertex v in vertices do
2:    v.parent ← nil
3:    if v = src then
4:       v.distance ← 0
5:    else
6:       v.distance ← ∞
7:    end if
8: end for
   //Edge relaxation
9: for i = 1 to size(vertices) − 1 do
10:   for all edge se in edges do
11:      Let vertex s = se.start
12:      Let vertex e = se.end
13:      if s.distance + se.cost < e.distance then
14:         e.distance ← s.distance + se.cost
15:         e.parent ← s
16:         e.flow ← min(s.flow, se.capacity)
17:      end if
18:   end for
19: end for
```

Lines 1-8 represent the initialization phase, where each node parent is set to nil, and the distance from the source node to all other nodes is set to infinity. Lines 9-19 represent the relaxation phase. Relaxation of edges encompasses looping on all vertices and at each iteration all edges are examined to see whether there is a shorter path to reach the current vertex or not. This algorithm is proved to have a worst case computation of $O(E.V)$ where E is the number of edges and V is the number of vertices.

Algorithm 2 keeps on augmenting paths (by calling getPath method) until the total augmented flow is zero, in this case the algorithm terminates. Augmenting a

Algorithm 2 Minimum Cost Maximum Flow algorithm.

```
1: while true do
2:    getPath(vertices, edges, source) {Call Bellmanford shortest path}
3:    pathflow ← dest.flow
4:    if pathflow = 0 then
5:       return
6:    end if
7:    current ← sink
8:    while current ≠ source do
9:       se.capacity ← se.capacity − pathflow {let se be the directed edge from
         current.parent to current}
10:      rev.capacity ← rev.capacity + pathflow {let rev be the reverse edge of se}
11:      current ← current.parent
12:   end while
13: end while
```

path subtracts a number of flow units from all edges on this path and add the same number of flow units to the reverse path, this helps doing reroutes as necessary, and prevents the algorithm from recalculating an already established path.

Chapter 4

Simulation and Performance Evaluation

This chapter describes the software simulation and experimental work that have been done to assess the performance of the proposed solution. This chapter presents the simulation environment setup such as supported system architecture, physical network layout, frequency planning model and SINR generation model. Simulation assumptions and general simulation parameters are mentioned in detail. Evaluation metrics and their respective simulation scenarios are also presented, along with scenario specific parameters. Simulation results and complexity analysis are shown towards the end of this chapter.

4.1 Simulation Setup

We built an in-house Java® based framework to simulate the different evaluation scenarios. We chose to develop an in-house simulator because at the time of this

decision, the available popular simulators like OPNET and NS-2 did not have available simulation modules for indoor small cells such as femtocells. We have chosen to develop our simulator using an industrial programming language because it supports high level of flexibility for writing, debugging and maintaining code. The simulation framework was built following a pluggable architecture, so that new algorithms can be added for comparison following simple steps.

4.1.1 System Topology

System Architecture

The system under simulation is an OFDMA network, composed of two tiers, namely macro-tier and femto-tier. The macro-tier encompasses a sole macrocell and a number of macrocell users, referred to as Macrocell User Equipments (MUEs). Whereas the femto-tier consists of a number of femtocells and their respective users. Femtocell users are referred to as Femtocell User Equipments (FUEs).

Physical Layout

Figure 4.1 shows the network layout of the simulated environment. The layout of the simulated network consists of:

- One FBS, referred to as: center femtocell, is placed at the origin.
- The MBS is placed at some distance North to the center femtocell.
- A number of FBSs are placed around the center femtocell in a random fashion.
- For each MBS or FBS, a number of UEs are randomly generated around the BS. An exception to this is the MBS, where users are generated in the direction of

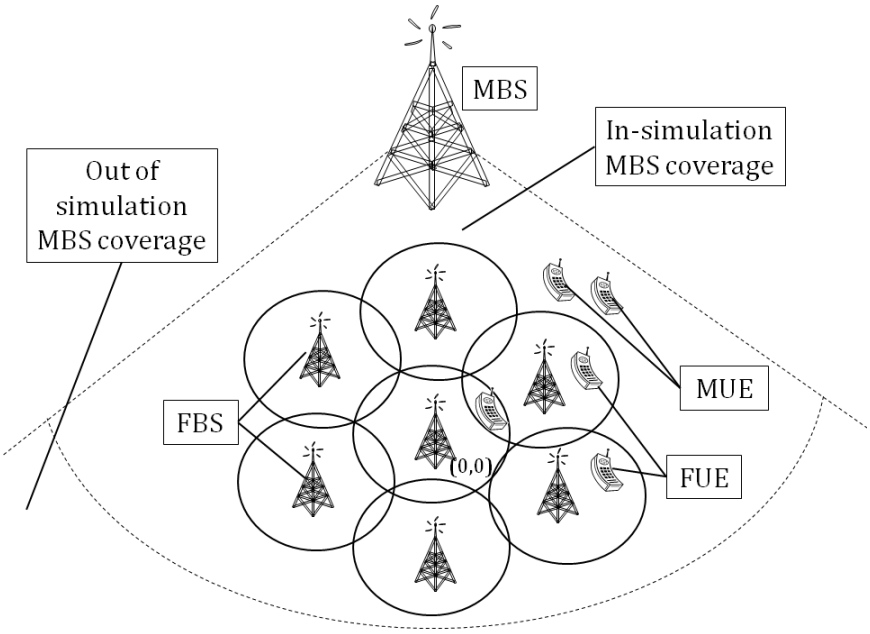

Figure 4.1: Physical layout of the simulated environment.

one sector only (120°), the sector facing the South direction. Only MUEs that are near FBSs are considered in this simulation, because MUEs that are away from the femto-tier do not cause or suffer major interference as near MUEs. And basically because the simulation is concerned with frequency allocation in the shared spectrum.

Frequency Planning Model

The frequency planning model used in the simulation is co-channel allocation. Where a certain frequency band is shared between femto-tier and macro-tier. This setup is adopted by operators who seek larger system capacity and can tolerate more interference in their networks. The frequency band is split into a number of subcarriers, which are grouped together to form RBs. RBs are considered the smallest units that

a UE can obtain, in terms of frequency allocation. Figure 3.1 shows an OFDMA downlink RB.

SINR Generation Model

The core of the simulation is based on the SINR experienced by every UE at each RB. SINR generation is based on the model proposed in [20] where a closed form modeling for the downlink SINR is presented. Using the antenna gains of a BS and a UE connected to it, transmission power of the BS and locations of interfering BSs as well as location of the UE, the authors have driven a Probability Density Function (PDF) for the downlink SINR conditioned on the location of a UE within a femtocell. Appendix A shows a brief derivation of how SINR is generated.

Simulation Assumptions

Certain conditions have been assumed when running the simulation experiments, these conditions are summarized below:

Transmission direction. A Downlink transmission system is assumed. This means that uplink traffic is neglected. In OFDMA downlink, the constraint of assigning contiguous RBs to a UE is relaxed. This provides some flexility and simplicity when implementing frequency allocation algorithms.

Fairness. The simulation works on a single SINR matrix, qualifying multiple algorithms against each other. A single SINR matrix affirms that fairness is not regarded. The aim is to maximize the overall system capacity by allowing different algorithms to make good assignment combinations. Handling fairness issues is recommended later as future work in section 5.3.

Parameter	Symbol	Value
Antenna Gain of BS	G_b	3 dBi
Antenna Gain of MS	G_m	0 dBi
Constant of path loss	C_s	43.8 dB
Path loss exponent on the link between a BS and a MS	α_j	3.6
MS Noise figure	φ	7 db
Channel Bandwidth	W	10 MHz
Central Frequency	f	5.25 GHz
Ambient Temprature	T	293 K
Number of Subcarriers per Resource Block	N_{SC}	12
Number of Resource Blocks	N_{RB}	50
Number of Femtocells	N_f	2-7
Number of users per femtocell j	N_{f_j}	3-5
Number of macrocell users	N_m	10-20
Transmission power of femtocell j	P_j	10-30 dBm
Transmission power of macrocell	P_m	43-46 dBm
Variance of shadow fading	σ_{X_s}	1-4
Distance between user i and femtocell j	D_{ij}	1-30 m
Distance between femtocell j and the center femtocell	D_j	10-50 m
Distance between the macrocell and the center femtocell	D_m	100-300 m
Distance between user i and the macrocell	D_{im}	50-200 m
Adjusting factor	β	ln(10)/10

Table 4.1: General Simulation Parameters

Central coordination. A central entity is assumed to be present. The role of this entity is to gather readings from different BSs and coordinate the frequency assignment to avoid collisions.

Simulation Parameters

Table 4.1 shows the simulation parameters used in all experiments. Some scenarios require fixing one or more of these parameters. Each of these scenarios will have a dedicated table with parameters that are assumed to have certain values throughout the scenario.

4.1.2 Candidate Algorithms

Chapter 2 provided a survey of recent works in the field of frequency allocation. The surveyed works covered the techniques used in such field. A number of schemes have been chosen to evaluate the performance of the proposed algorithm. These schemes have been implemented to the best of our knowledge, to carry out the functions intended originally by their authors in the referenced papers. We carefully chose the closest techniques to our proposed scheme. We prioritized schemes that depended on channel allocation over schemes that depended on power allocation. We were also keen to choose schemes that are easy to implement in order not to miss any detail that might compromise fairness in our simulation. The next section shows the results of our choice.

4.1.3 Kim's Algorithm

In [12], Kim et al. proposed a centralized, system capacity maximization algorithm. The algorithm is two-fold: 1. Power allocation phase, and 2. Sub-channel allocation phase. To match the objective function of this scheme with the proposed MCF, only the sub-channel allocation part has been implemented. To maintain the simulation assumptions in [20], transmission power of a BS is kept constant throughout a single experiment. Two versions of this algorithm have been developed: a CSG version, to match the simulation assumptions for the proposed MCF algorithm, and another Open Subscriber Group (OSG) version to fully exploit the strength of Kim's algorithm. The difference between the two versions is that in a CSG environment, users are pre-attached to their BSs, and hence, users are allocated RBs at the serving BS. Whereas in the OSG version, a UE is allowed to switch to a better serving BS by means of

handover. The OSG version is referred to as Kim09OSG, and the CSG version is referred to as Kim09CSG. These notations are used throughout the simulation and performance evaluation. Algorithm 3 shows the CSG of Kim's algorithm (Kim09CSG). We compared both versions with the proposed MCF scheme, and the results are shown in section 4.2.

Pseudo-code

Algorithm 3 Kim09CSG algorithm.

Let $rate$ be the required user rate in units of RBs.
Let $\Gamma_{N,R}$ be the SINR matrix of N UEs versus R RBs.
Let $allocated$ be an integer array of size N.
for all r **do**
    Find the best $\gamma_{n,r} \in \Gamma$ where $allocated[n] < rate$
    $allocated[n] \leftarrow allocated[n] + 1$ {Assign RB r to UE n}
end for

4.1.4 In-house Greedy Solution

We have devised a greedy based approach to compare the proposed solution against. Fairness was not put into consideration, to guarantee unified simulation assumptions. The greedy approach works on the same SINR matrix which the MCF works on. It starts out by sorting all the values in the matrix in a descending order. And given the number of RB required by each UE, the algorithm starts crossing out SINR values from top to bottom, maintaining the condition that no two UEs share a RB, and keeps assigning RBs to UEs until each UE get its required RBs. Algorithm 4 shows a pseudo-code for the in-house greedy algorithm.

Pseudo-code

Algorithm 4 In-house Greedy Algorithm.

Let $rate$ be the required user rate in units of RBs.
Let $\Gamma_{N,R}$ be the SINR matrix of N UEs versus R RBs.
Let $allocated$ be an integer array of size N.
Let $booked$ be a boolean array of size R.
sort(Γ) {Sort the SINR matrix in descending order}
for all n **do**
    $allocated[n] \leftarrow 0$
end for
for all r **do**
    $booked[r] \leftarrow false$
end for
for all $\gamma_{n,r}$ in Γ **do**
    if $allocated[n] < rate$ and $booked[r] = false$ **then**
        $allocated[n] \leftarrow allocated[n] + 1$ {Assign RB r to UE n}
        $booked[r] \leftarrow true$ {Mark RB r as used}
    end if
end for

4.2 Simulation Results

This section presents a number of performance metrics that have been established to assess the performance of the proposed algorithm versus other schemes. Each metric is measured by implementing one or more scenarios. The results of running these scenarios will be presented in graphical format to aid the reader in concluding them.

4.2.1 Capacity Metric

Capacity is regarded as the theoretical system throughput that can be achieved. Given a certain assignment of RBs to UEs. Capacity C for an assignment is calculated as $B\sum_{r}\sum_{p=1}^{P}\log_2(1+\gamma_{rp})$. Where B is the physical bandwidth in Hz, r is a RB assigned to a user, P is the number of subcarriers per RB, and γ_{rp} is the SINR of the p^{th} subcarrier in RB r.

Experiment A1: Effect of changing number of users per femtocell

In this experiment, capacity is evaluated in response to changing the number of users per femtocell. The experiment has been repeated 20 times per each value from the set [1, 2, 3, 4, 5]. Table 4.2 identifies the experiment specific parameters that differ from the general simulation parameters presented in table 4.1.

Parameter	Symbol	Value
Number of users per femtocell j	N_{f_j}	[1, 2, 3, 4, 5]
Number of Femtocells	N_f	7
Number of macrocell users	N_m	15

Table 4.2: Experiment A1 specific parameters.

For each experiment run with a certain seed, all capacities attained from all schemes are normalized relative to 100, i.e. the capacity value of the algorithm that scores best is set to 100, and capacities from other algorithms are set to a percentage of the best capacity, as in equation 4.1. Then, for each value of N_{f_j}, all normalized capacities are averaged as in equation 4.2

$$\text{Normalized capacity at seed } s = \frac{\text{Capacity at seed } s}{\text{Best capacity at seed } s} * 100 \tag{4.1}$$

$$\text{Normalized capacity at a certain value } N_{f_j} = \frac{\sum_s \text{Normalized capacity at seed } s}{20} \tag{4.2}$$

Figure 4.2 shows the simulation results of experiment A1. The proposed optimal algorithm, MCF, outperforms all other schemes as expected. The in-house greedy approach scores near optimal capacity, 0.5% to 1.0% less performance than optimal.

Kim09OSG and Kim09CSG scored alternating results at 3.5% to 6.0% less performance than optimal. The reason behind the near optimal performance of the in-house greedy approach is the data distribution of SINR values. Typically, a UE will experience slightly varying SINR values per each RB. Hence, choosing greedily to assign a certain RB to a UE will not incur a huge cost in terms of blocking another UE to use the same RB if it results in a total higher capacity. If the SINR distribution was more diverse, performance problems would arise from using greedy schemes.

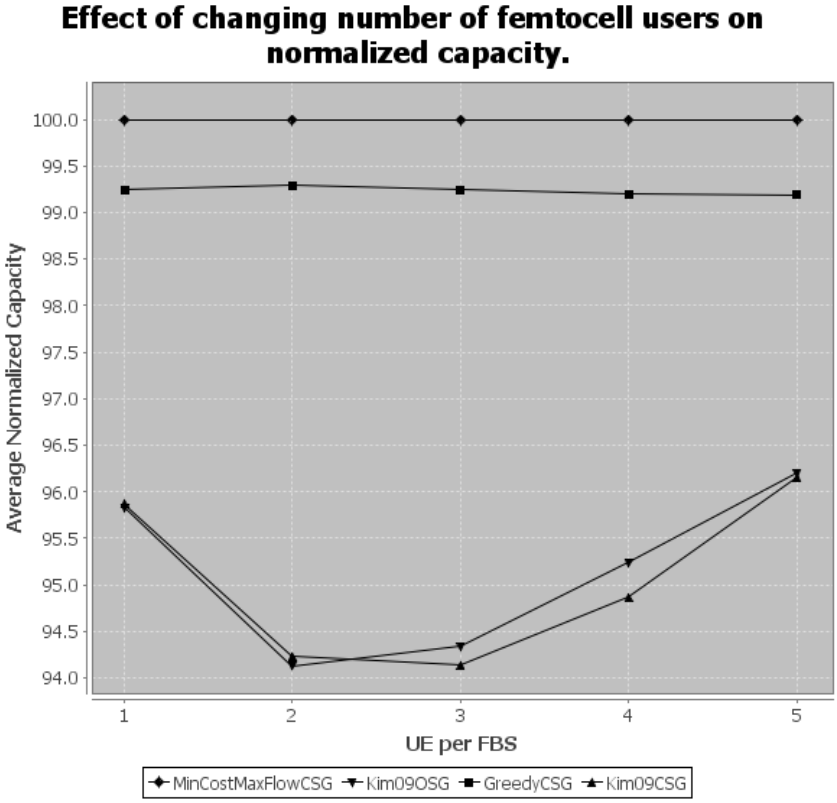

Figure 4.2: Experiment A1: Average Normalized Capacity vs. changing number of users per femtocell.

Experiment B1: Effect of changing the total number of serving FAPs

In experiment B1, capacity is evaluated against changing the total number of serving femtocells, while keeping the number of users constant. The experiment has been repeated 20 times per each value from the set [1, 2, 3, 4]. Table 4.3 shows the experiment specific parameters that differ from the general simulation parameters presented in table 4.1.

Parameter	Symbol	Value
Number of Femtocells	N_f	[1, 2, 3, 4]
Total number of FUEs	$\sum N_{f_j}$	24
Number of users per femtocell j	N_{f_j}	[24, 12, 8, 6]
Number of macrocell users	N_m	26

Table 4.3: Experiment B1 specific parameters.

For each value for the number of femtocells, N_f, the total number of femtocell users is split equally among the number of femtocells. Which is why the total number of FUEs was chosen to be 24, a multiple of all candidate values of N_f.

As presented in experiment A1. Capacities of all algorithms are calculated and normalized per each seed value, as in equation 4.1. Then, averaged for each value of N_f as in equation 4.3.

$$\text{Normalized capacity at a certain value } N_f = \frac{\sum_s \text{Normalized capacity at seed } s}{20} \tag{4.3}$$

The results of experiment B1 are shown in figure 4.3. MCF still outperforms the other schemes. The in-house greedy approach comes next at 99% to 99.5% optimal performance. Whereas, Kim09OSG and Kim09CSG scored alternating results at 95%

to 97.5% optimal performance.

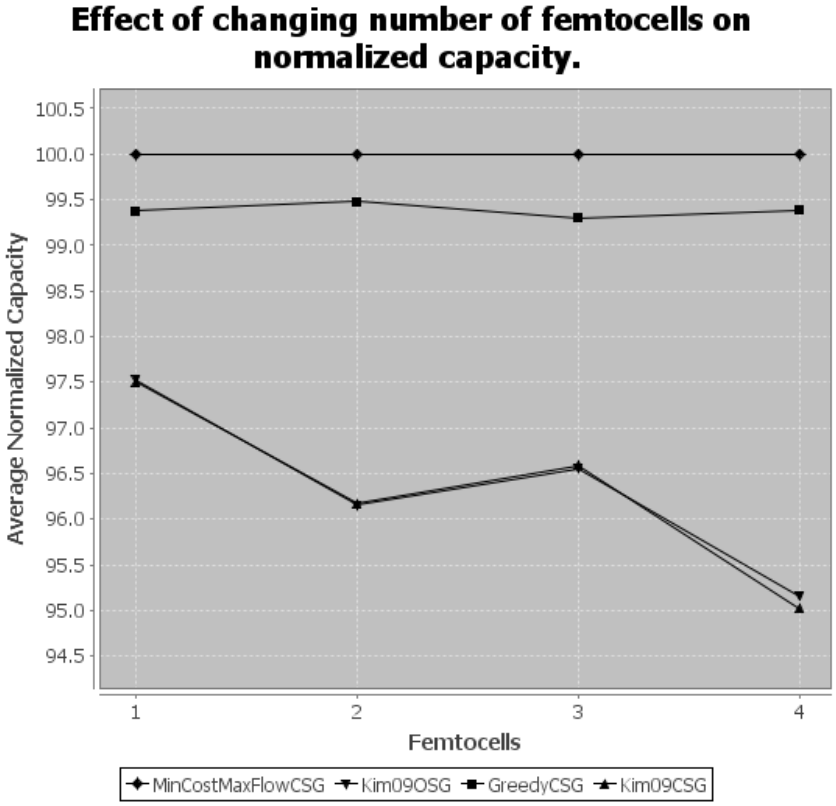

Figure 4.3: Experiment B1: Average Normalized Capacity vs. changing number of femtocells.

Experiment C1: Effect of User Mobility

In experiment C1, capacity is calculated to assess the effect of user mobility on the algorithms in comparison. A simple Random Waypoint (RWP) mobility model was applied. Across the interval of 50 iterations, each UE may randomly move to another position. The new position can be one meter away in the horizontal direction, and/or one meter away in the vertical direction, from the old position. Table 4.4 shows the experiment specific parameters that differ from the general simulation parameters

presented in table 4.1.

Parameter	Symbol	Value
Number of Femtocells	N_f	4
Number of users per femtocell j	N_{f_j}	4
Total number of FUEs	$\sum N_{f_j}$	16
Number of macrocell users	N_m	9

Table 4.4: Experiment C1 specific parameters.

As seen in table 4.4, the number of FUEs is 16, and the number of MUEs is 9, for a total of 25 UEs. This results in two RBs per user.

The layout generation is done once at the beginning of this experiment. And the positions of all UEs are updated at each iteration, by applying RWP mobility model, as explained. The SINR matrix is calculated at each iteration as well, before the algorithms run again for this iteration.

The results of experiment C1 are shown in figure 4.4. The proposed benchmark MCF stays at the top, while the in-house greedy approach is just below it at 98.5% to 99.7% optimal performance. Kim09OSG and Kim09CSG fluctuate around 95.5% to 98% optimal performance.

In the experiments above, although a greedy scheme performed quite well versus the optimal scheme, the other two approaches namely; Kim09OSG and Kim09CSG did not reach such performance. The main drawback in Kim's approach proposed in [12] is that it deals with one RB at a time, trying to maximize the benefit (capacity in this case) from using this RB. The problem is that a UE can be sufficiently served from earlier RBs, leaving out better capacity RBs that might come later, and probably wasting good RBs on other UEs. This flaw in Kim's approach did not let it benefit fully from being a greedy-based scheme.

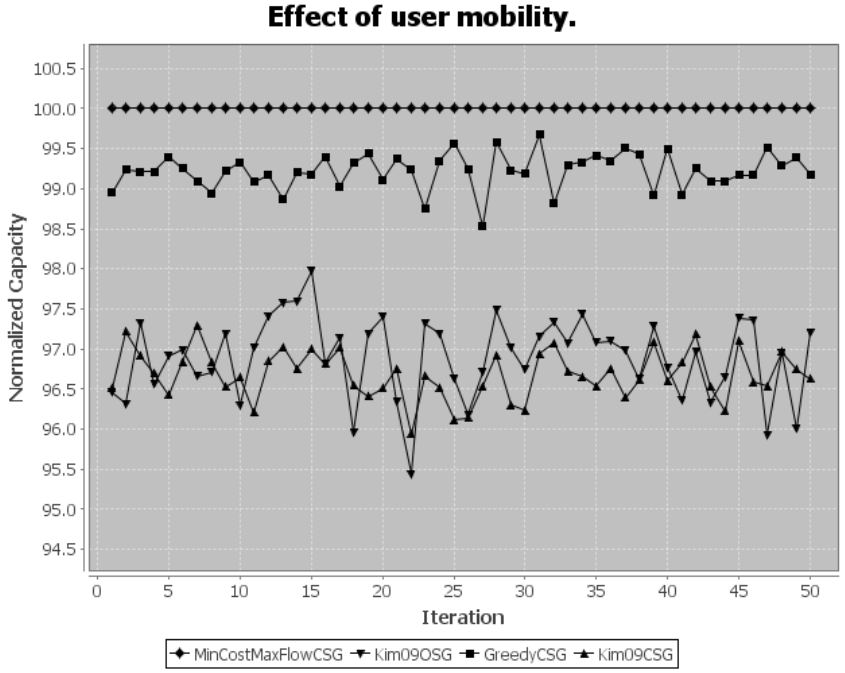

Figure 4.4: Experiment C1: Effect of applying Random Waypoint mobility model on the normalized capacity.

4.2.2 Elapsed Time Metric

To further elaborate on the practicality of the proposed solution and the other schemes; experiment A1, which was targetted towards capacity calculation, was repeated again. Time in milliseconds was recorded for each experiment and averaged per user value N_{f_j}. Figure 4.5 shows the average time elapsed per user value, in milliseconds. Section 4.3 provides complexity analysis as a means of supporting the results.

Clearly, the optimal MCF takes more time undergoing calculations to achieve optimality. The in-house greedy scheme, comes in the second place with much lower complexity and time, whereas the two versions of Kim's algorithm score the best performance due to their relatively low complex nature.

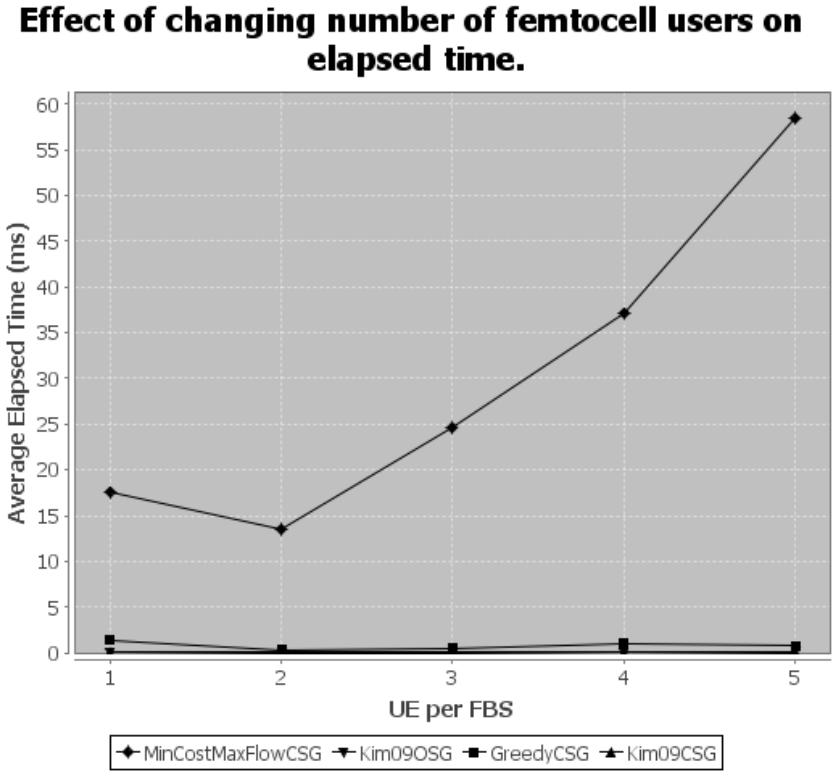

Figure 4.5: Experiment A2: Average Elapsed Time.

4.3 Complexity and Performance Analysis

This section presents a complexity and performance analysis of the algorithms used in the simulation.

The complexity of every used scheme is derived in the following section. Table 4.5 presents the result of complexity and performance analysis, which will be used in the conclusion of this thesis. The average run times from experiment A2 are also added to table 4.5 to aid in the comparison. For the purpose of runtime complexity analysis, let N be the total number of UEs, including FUEs and MUEs, and let R be the total number of RBs available.

MCF Complexity

Algorithm 2 runs in iterations. It finds a shortest path in every iteration, assigning a RB to a user, possibly reassigning another RB if needed. This makes the outer loop of $O(R)$ complexity. The call to Bellmanford shortest path depicted in Algorithm 1 has a worst case complexity of $O(V.E)$ where V is the size of *vertices* list and E is the size of *edges* list. Since the generated graph is fully connected then $V = R + N + 2$ and $E = R.N + R + N$. Essentially, this comes from R RBs, each one is connected to N UEs, in addition to N links to the artificial source and R links to the artificial sink. Note that the dominant term is $R.N$.

Hence the total complexity of a MCF based on Bellmanford shortest path is $O(R.(R + N).(R.N)) = O(R^2.N(R + N))$

Kim's Algorithm Complexity

The complexity analysis of algorithm 3 is pretty straight forward. It encompasses R loops on all RBs, each has a maximum of N UEs to check. This brings the algorithm to a complexity of $O(N.R)$. Similarly, the OSG version of this algorithm, referred to as Kim09OSG, is $O(N.R.B)$, where B is the number of BSs.

Greedy In-house Scheme Complexity

Algorithm 4 starts by sorting out the SINR matrix, typically with complexity $O(N.R)\log(N.R)$. The loop in lines 11-17 is of $O(N.R)$. Since sorting is the dominating factor then the algorithm complexity is of $O(N.R)\log(N.R)$

Based on the results in table 4.5, recommendations will be provided in chapter 5, which concludes this thesis.

Algorithm	Complexity	Average Runtime (ms)
MCF	$O\left(R^3.N + R^2.N^2\right)$	10s of ms
In-house Greedy	$O\left(N.R.\log(N.R)\right)$	1 ms
Kim09CSG	$O\left(R.N\right)$	< 1 ms

Table 4.5: Complexity analysis of the algorithms in simulation.

	$RB1$	$RB2$
UEA	10.9	10.5
UEB	10.8	1.0

Figure 4.6: Corner case challenging the greedy approach.

4.4 A Note on The Achieved Results

It may be arguable that the achieved results may not justify the MCF complexity, despite the fact that it is optimal and the running time is very reasonable. We would like to note that the achieved results are based on the data distribution of the generated SINR values. For the sake of integrity, we are using the same method to generate SINR values as in [20]. Lab simulations of MCF have proven that in cases where SINR values differ greatly per UE, the performance gain can be as high as 50%, or higher according to the discrepancy in SINR levels. The trivial example in Figure 4.6 shows the SINR values that two UEs, A and B, experience against two RBs. A standard greedy algorithm will choose to assign RB-1 to UE-A and hence RB-2 will be assigned to UE-B, resulting in a total SINR of $10.9 + 1.0 = 11.9$. The MCF, on the other hand, will choose the best configuration, which assigns RB-2 to UE-A, and RB-1 to UE-B, resulting in a total SINR of $10.5 + 10.8 = 21.3$

Chapter 5

Summary and Conclusion

5.1 Summary

In this thesis we presented an introduction to femtocell networks and highlighted the essence of establishing them. We also stressed that the application of newer networks like LTE and LTE Advanced will require the existence of femtocells as a step towards the logical evolution of small and personal BSs. We also presented the interference problem in detail, and the importance of mitigation solutions in smooth service provisioning.

We leveraged a representative set of proposals from the literature to combat interference. Several solutions exist that vary in nature (centralized versus distributed) and at the level at which the solution is applied (femtocellular, femtocellular / macrocellular). Some solutions resort to transmission power management while others utilizes frequency allocation. A comparison of some of these solutions was presented in chapter 2. Also, we proposed a novel and effective algorithm to address a definite void in the literature to tackle outstanding problems in interference mitigation.

We emphasize on the importance of interference mitigation to guarantee the expected return from femtocell networks. The use of highly efficient algorithms has been already proposed in the literature to complement traditional methods that rely on pure optimizations to either the physical or the MAC layers. In [40] the need for non-conventional network planning and optimization techniques has been motivated, with assertions that distributed, self-optimized techniques are anticipated to produce more reliable results than ordinary algorithms [15].

When multiple operators come into play [51], and with the introduction of LTE networks and the notions of virtualization, 'global spectrum' [52], and cognitive radio [53], very high level of coordination is required to guarantee smooth operation for all operators. A new class of cooperative techniques will emerge to cope with this new network architecture [53, 54]. At the same time, self-optimization on the cell level will be a critical feature to have because FBSs will no longer come from the same provider, in addition to the large number of small cells introduced by femtocell technology.

Heterogeneous Networks (HetNets) [17, 35, 55], a recently introduced evolutionary notion of networking, have been establishing the importance of cooperative multi-operator environment. A HetNet comprises a number of mixed macrocells, remote radio heads and low-power nodes such as picocell and femtocells. Main characteristics of the HetNet architecture include: high degree of spatial reuse, enhanced indoor coverage, and highly technically challenging environment [18]. Such environment demonstrates a number of interference sources, for example: unplanned deployment, power difference between nodes, and range expanded users.

5.2 Conclusion

We presented the results of extensive simulations to assess the quality of the proposed solution. Despite the outstanding results that the proposed solution demonstrated against representatives from the literature, we confidently see that a carefully optimized greedy algorithm will be sufficient - although not optimal - to use. Even with lots of greedy based algorithms in the literature, the way the algorithm is devised and coded makes a difference.

Chapter 4 shows the results of lab simulations that made us reach the conclusion that although greedy is not optimal, but greedy is good. As long as channel models follow certain non-random distributions, greedy performance will be the most acceptable in terms of quality and complexity. Simulations showed that a carefully coded greedy approach scored a performance of 99% optimal. Moreover, operators still have the liberty to choose to achieve the remaining 1% at the extra small cost of complexity, using algorithms like the proposed MCF.

5.3 Recommendations and Future Work

Certain constraints have been assumed when running the experimental simulation as elaborated in section 4.1. These constraints were assumed to make the simulation more focused and easier in implementation. However, in a real scenarios these restrictions cease to exist. And the less constraints a simulation assumes, the more realistic it is. This section provides some recommendations to overcome the simulation assumptions, and can be considered as future work.

5.3.1 Fairness Issues

As presented, MCF works on a two dimensional matrix of numbers, maximizing the summation of values, under certain constraints. MCF in its core does not regard the locations of the chosen values within the SINR mtarix. Hence, constraints are put to limit the number of RBs per UE. However, as seen throughout this thesis, fairness is totally ignored. We developed a recommendation based on Proportional Fairness algorithms, to incorporate fairness in a MCF. The idea is to apply a fairness factor on the SINR matrices at subsequent frames, to force a UE that has been served relatively more than other UEs, to have its SINR levels reduced by some factor proportional. This reduction factor is directly proportional to the amount of admission this UE has gained.

5.3.2 Adding Support to Uplink

The proposed scheme was targetted to downlink only, because downlink frequency assignment is easier to deal with due to the fact that assigned resources don't have to be contiguous. There is a number of tricks in MCF implementation that allows adding specific constraints to the resulting assignment. For example, in a MCF graph, controlling the flow values on the links from the artificial source to the UEs, controls how many flow units can move through a certain UE node, or in other words control how many RBs can be assigned. We have been investigating tweaks on the regular MCF to add support of uplink transmission as well, however, at the time of writing the thesis, these tweaks were not mature enough to report.

5.3.3 Distributed Operation

The proposed scheme in this thesis assumes centralized operation. It assumes the existence of a centralized entity that gathers SINR information from BSs and handle frequency assignment properly to avoid collision. The amount of signalling needed to interface with the centralized entity may be in some cases costly or intolerable. This urges the development of a distributed version of the proposed scheme. In [19], the authors propose a decentralized hashing algorithm to aid in identifying nodes in a network in a distributed fashion. They provide a collision resolution mechanism as well. This scheme can be incorporated with MCF to provide a distributed optimal scheme.

Bibliography

[1] International Telecommunications Union, "Key global telecom indicators for the world telecommunication service sector." `http://www.itu.int/ITU-D/ict/statistics/at_glance/KeyTelecom.html`.

[2] S. Saunders, S. Carlaw, A. Giustina, R. R. Bhat, V. S. Rao, and R. Siegberg, *Femtocells: Opportunities and Challenges for Business and Technology*. New York, NY, USA: John Wiley and Sons, 2009.

[3] E. Dahlman, S. Parkvall, J. Skold, and P. Beming, *3G Evolution, Second Edition: HSPA and LTE for Mobile Broadband*. Academic Press, 2008.

[4] M.-S. Alouini and A. Goldsmith, "Area Spectral Efficiency of Cellular Mobile Radio Systems," vol. 2, pp. 652–656, May 1997.

[5] X. Chu, Y. Wu, L. Benmesbah, and W.-K. Ling, "Resource Allocation in Hybrid Macro/Femto Networks," in *Wireless Communications and Networking Conference Workshops (WCNCW), 2010 IEEE*, pp. 1–5, April 2010.

[6] Y. Bai, J. Zhou, and L. Chen, "Hybrid Spectrum Usage for Overlaying LTE Macrocell and Femtocell," *GLOBECOM 2009 - 2009 IEEE Global Telecommunications Conference*, pp. 1–6, November 2009.

[7] M. Dohler, R. Heath, A. Lozano, C. Papadias, and R. Valenzuela, "Is the PHY Layer Dead?," *Communications Magazine, IEEE*, vol. 49, pp. 159–165, April 2011.

[8] J. Hoydis, M. Kobayashi, and M. Debbah, "Green Small-Cell Networks," *Vehicular Technology Magazine, IEEE*, vol. 6, pp. 37–43, March 2011.

[9] J. Zhang, G. D. L. Roche, and G. L. D. Roche, *Femtocells: Technologies and Deployment*. John Wiley and Sons, Ltd., 2010.

[10] D. Lopez-Perez, A. Valcarce, and G. de La Roche, "OFDMA femtocells: A roadmap on interference avoidance," *IEEE Communications Magazine*, vol. 47, pp. 41–48, September 2009.

[11] J. Cullen, "Radioframe presentation," *Femtocells Europe*, June 2008.

[12] J. Kim and D.-H. Cho, "A Joint Power and Subchannel Allocation Scheme Maximizing System Capacity in Dense Femtocell Downlink Systems," in *Personal, Indoor and Mobile Radio Communications, 2009 IEEE 20th International Symposium on*, pp. 1381–1385, September 2009.

[13] D. Knisely, T. Yoshizawa, and F. Favichia, "Standardization of Femtocells in 3GPP," *Communications Magazine, IEEE*, vol. 47, pp. 68–75, September 2009.

[14] S. Carlaw, "IPR and The Potential Effect on Femtocell Markets," *Femtocells Europe*, June 2008.

[15] J.-H. Yun and K. Shin, "Adaptive Interference Management of OFDMA Femtocells for Co-Channel Deployment," *Selected Areas in Communications, IEEE Journal on*, vol. 29, pp. 1225–1241, June 2011.

[16] "Merrill Lynch. Wireless data growth: How far, how fast, and who wins?," tech. rep., Merrill Lynch, 2007.

[17] S.-M. Cheng, S.-Y. Lien, F.-S. Chu, and K.-C. Chen, "On Exploiting Cognitive Radio to Mitigate Interference in Macro/Femto Heterogeneous Networks," *Wireless Communications, IEEE*, vol. 18, pp. 40–47, June 2011.

[18] D. Lopez-Perez, I. Guvenc, G. de la Roche, M. Kountouris, T. Quek, and J. Zhang, "Enhanced Intercell Interference Coordination Challenges in Heterogeneous Networks," *Wireless Communications, IEEE*, vol. 18, pp. 22–30, June 2011.

[19] K. Sundaresan and S. Rangarajan, "Efficient resource management in ofdma femto cells," in *Proceedings of the tenth ACM international symposium on Mobile ad hoc networking and computing*, MobiHoc '09, (New York, NY, USA), pp. 33–42, ACM, 2009.

[20] K. W. Sung, H. Haas, and S. McLaughlin, "A Semianalytical PDF of Downlink SINR for Femtocell Networks," *EURASIP Journal on Wireless Communications and Networking*, vol. 2010, pp. 1–10, 2010.

[21] H. Hristov, R. Feick, and W. Grote, "Improving indoor signal coverage by use of through-wall passive repeaters," in *Antennas and Propagation Society International Symposium, 2001. IEEE*, vol. 2, pp. 158 –161 vol.2, 2001.

[22] V. Chandrasekhar, J. Andrews, and A. Gatherer, "Femtocell Networks: A Survey," *Communications Magazine, IEEE*, vol. 46, pp. 59–67, September 2008.

[23] T. Nihtila, "Increasing Femto Cell Throughput with HSDPA Using Higher Order Modulation," in *Networking and Communications Conference, 2008. INCC 2008. IEEE International*, pp. 49–53, May 2008.

[24] H. Claussen, "Performance of Macro- and Co-Channel Femtocells in a Hierarchical Cell Structure," in *Personal, Indoor and Mobile Radio Communications, 2007. PIMRC 2007. IEEE 18th International Symposium on*, pp. 1–5, September 2007.

[25] G. Korinthios, E. Theodoropoulou, N. Marouda, I. Mesogiti, E. Nikolitsa, and G. Lyberopoulos, "Early Experiences and Lessons Learned from Femtocells," *Communications Magazine, IEEE*, vol. 47, pp. 124–130, September 2009.

[26] K. Kim and C. Wang, "Enterprise voip in fixed mobile converged networks," in *Multimedia Analysis, Processing and Communications* (W. Lin, D. Tao, J. Kacprzyk, Z. Li, E. Izquierdo, and H. Wang, eds.), vol. 346 of *Studies in Computational Intelligence*, pp. 585–621, Springer Berlin / Heidelberg, 2011.

[27] M. Krichen, J. Cohen, and D. Barth, "File transfer application for sharing femto access," *CoRR*, vol. abs/1104.5150, 2011.

[28] H. Aki, M. C. Erturk, and H. Arslan, "Dynamic channel allocation schemes for overlay cellular architectures," in *Proceedings of the 9th conference on Wireless telecommunications symposium*, WTS'10, (Piscataway, NJ, USA), pp. 67–71, IEEE Press, 2010.

[29] T. Kahwa and N. Georganas, "A Hybrid Channel Assignment Scheme in Large-Scale, Cellular-Structured Mobile Communication Systems," *Communications, IEEE Transactions on*, vol. 26, pp. 432–438, April 1978.

[30] J. Sin and N. Georganas, "A Simulation Study of a Hybrid Channel Assignment Scheme for Cellular Land-Mobile Radio Systems with Erlang-C Service," *Communications, IEEE Transactions on*, vol. 29, pp. 143–147, February 1981.

[31] W. Yue, "Analytical methods to calculate the performance of a cellular mobile radio communication system with hybrid channel assignment," *Vehicular Technology, IEEE Transactions on*, vol. 40, pp. 453–460, May 1991.

[32] I. Guvenc, M.-R. Jeong, F. Watanabe, and H. Inamura, "A Hybrid Frequency Assignment for Femtocells and Coverage Area Analysis for Co-channel Operation," *Communications Letters, IEEE*, vol. 12, pp. 880–882, December 2008.

[33] Y. Bai, J. Zhou, and L. Chen, "Hybrid Spectrum Sharing for Coexistence of Macrocell and Femtocell," in *Communications Technology and Applications, 2009. ICCTA '09. IEEE International Conference on*, pp. 162–166, October 2009.

[34] M. Bennis, L. Giupponi, E. Diaz, M. Lalam, M. Maqbool, E. Strinati, A. De Domenico, and M. Latva-aho, "Interference Management in Self-organized Femtocell Networks: The BeFEMTO Approach," in *Wireless Communication, Vehicular Technology, Information Theory and Aerospace Electronic Systems Technology (Wireless VITAE), 2011 2nd International Conference on*, pp. 1–6, March 2011.

[35] S.-P. Yeh, S. Talwar, G. Wu, N. Himayat, and K. Johnsson, "Capacity and Coverage Enhancement in Heterogeneous Networks," *Wireless Communications, IEEE*, vol. 18, pp. 32–38, June 2011.

[36] R.-T. Juang, P. Ting, H.-P. Lin, and D.-B. Lin, "Interference Management of Femtocell in Macro-cellular Networks," in *Wireless Telecommunications Symposium (WTS), 2010*, pp. 1–4, April 2010.

[37] H.-C. Lee, D.-C. Oh, and Y.-H. Lee, "Mitigation of Inter-Femtocell Interference with Adaptive Fractional Frequency Reuse," in *Communications (ICC), 2010 IEEE International Conference on*, pp. 1–5, May 2010.

[38] T. Lee, H. Kim, J. Park, and J. Shin, "Dynamic fractional-frequency reuse for femtocells," in *Proceedings of the 5th International Conference on Ubiquitous Information Management and Communication*, ICUIMC '11, (New York, NY, USA), pp. 80:1–80:6, ACM, 2011.

[39] F. Mazzenga, M. Petracca, R. Pomposini, F. Vatalaro, and R. Giuliano, "Algorithms for Dynamic Frequency Selection for Femto-cells of Different Operators," in *Personal Indoor and Mobile Radio Communications (PIMRC), 2010 IEEE 21st International Symposium on*, pp. 1550–1555, September 2010.

[40] T. Akbudak and A. Czylwik, "Distributed Power Control and Scheduling for Decentralized OFDMA Networks," in *Smart Antennas (WSA), 2010 International ITG Workshop on*, pp. 59–65, February 2010.

[41] Z. Bharucha, A. Saul, G. Auer, and H. Haas, "Dynamic resource partitioning for downlink femto-to-macro-cell interference avoidance," *EURASIP Journal on Wireless Communications and Networking*, vol. 2010, pp. 2:1–2:12, January 2010.

[42] G. E. M. Zhioua, P. Godlewski, S. Hamouda, and S. Tabbane, "Quietest channel selection for femtocells in ofdma networks," in *Proceedings of the 8th ACM*

international workshop on Mobility management and wireless access, MobiWac '10, (New York, NY, USA), pp. 125–128, ACM, 2010.

[43] H. Claussen, L. Ho, and L. Samuel, "Self-optimization of Coverage for Femtocell Deployments," in *Wireless Telecommunications Symposium, 2008. WTS 2008*, pp. 278–285, April 2008.

[44] N. Arulselvan, V. Ramachandran, S. Kalyanasundaram, and G. Han, "Distributed Power Control Mechanisms for HSDPA Femtocells," in *VTC Spring 2009 - IEEE 69th Vehicular Technology Conference*, pp. 1–5, April 2009.

[45] E. J. Hong, S. Y. Yun, and D.-H. Cho, "Decentralized Power Control Scheme in Femtocell Networks: A Game Theoretic Approach," in *Personal, Indoor and Mobile Radio Communications, 2009 IEEE 20th International Symposium on*, pp. 415–419, September 2009.

[46] C.-W. Chen, C.-Y. Wang, S.-L. Chao, and H.-Y. Wei, "Dance: a game-theoretical femtocell channel exchange mechanism," *ACM SIGMOBILE Mobile Computing and Communications Review*, vol. 14, pp. 13–15, July 2010.

[47] V. Chandrasekhar, J. Andrews, T. Muharemovic, Z. Shen, and A. Gatherer, "Power Control in Two-tier Femtocell Networks," *Wireless Communications, IEEE Transactions on*, vol. 8, pp. 4316–4328, August 2009.

[48] M. Sahin, I. Guvenc, M.-R. Jeong, and H. Arslan, "Handling CCI and ICI in OFDMA Femtocell Networks Through Frequency Scheduling," *Consumer Electronics, IEEE Transactions on*, vol. 55, pp. 1936–1944, November 2009.

[49] R. K. Ahuja, T. L. Magnanti, and J. B. Orlin, *Network Flows: Theory, Algorithms, and Applications*. Englewood Cliffs, NJ: Prentice Hall, 1993.

[50] D. B. West, *Introduction to Graph Theory (2nd Edition)*. Prentice Hall, Aug. 2000.

[51] F. Mazzenga, M. Petracca, R. Pomposini, and F. Vatalaro, "Improving qos of femtocells in multi-operator environments," in *Trustworthy Internet* (L. Salgarelli, G. Bianchi, and N. Blefari-Melazzi, eds.), pp. 117–128, Springer Milan, 2011.

[52] E. K. Paik, S.-H. Lee, C. Lee, J. Han, C. Park, T. Kwon, and Y. Choi, "Service Differentiation Using Mobile Femtocell Virtualization," in *Consumer Communications and Networking Conference (CCNC), 2010 7th IEEE*, pp. 1–4, January 2010.

[53] R. Urgaonkar and M. J. Neely, "Opportunistic Cooperation in Cognitive Femtocell Networks," *ArXiv e-prints*, March 2011.

[54] K. Lee, O. Jo, and D.-H. Cho, "Cooperative Resource Allocation for Guaranteeing Intercell Fairness in Femtocell Networks," *Communications Letters, IEEE*, vol. 15, pp. 214–216, February 2011.

[55] H. Li, J. Hajipour, A. Attar, and V. Leung, "Efficient HetNet Implementation Using Broadband Wireless Access with Fiber-connected Massively Distributed Antennas Architecture," *Wireless Communications, IEEE*, vol. 18, pp. 72–78, June 2011.

Appendix A

Derivation of SINR PDF

This appendix provides a summary to the derivation of the downlink SINR matrix as demonstrated in [20]. In short the authors calculate three PDFs to derive the PDF of downlink SINR. The three PDFs are:

1. The PDF for the power received at a UE.
2. The PDF of the aggregated interference received at the same UE.
3. The PDF of the background noise value.

Given a BS at the center of a cell, call it Cell of Interest (CoI). The cell has a radius R, and M UEs uniformly distributed within the radius of this cell. Without loss of generality, the CoI can be assumed to be placed at the origin (0, 0). Using this, an arbitrary UE m is located at (r_m, r_θ) where $0 \leq r_m \leq R$ and $0 \leq r_\theta \leq 2\pi$. Also, the location of the jth interfering BS would be $(r_b(j), \theta_b(j))$.

To calculate the power received at UE m:

- P_s^t: transmission power of the BS at the CoI.

- G_b: antenna gain of the BS at the CoI, G_m: the antenna gain of the UE.
- C_s: constant of path loss in the CoI.
- α_s: path loss exponent of the CoI.
- X_S: Gaussian random variable modeling the shadow fading, with zero mean and $\sigma^2_{X_s}$ variance in db.
- β: $\dfrac{\ln 10}{10}$.

The received signal power at UE m from the serving BS will be

$$P^r_s = P^t_s G_b G_m C_s r_m^{-\alpha_s} \exp(\beta X_s)$$

which can also be written as

$$P^r_s = \exp\left[\ln(P^t_s G_b G_m C_s) - \alpha_s \ln r_m + (\beta X_s)\right]$$

which follows a log-normal distribution [20], and thus the PDF conditional on the location of the UE m is given by

$$f_{p^r_s}(z \,|\, r_m,\, \theta_m) \;= \frac{1}{z\sigma_s\sqrt{2\pi}} \exp\left[\frac{-(\ln z - \mu_s)^2}{2\sigma_s^2}\right] \tag{A.1}$$

where $\mu_s = \ln(P^t_s G_b G_m C_s) - \alpha_s \ln r_m$ and $\sigma_s^2 = \beta^2 \sigma^2_{X_s}$.

To calculate the interference at a UE m:

- P^t_j: transmission power from the jth BS.

- C_j: path loss constant on the link between jth BS and UE m.
- α_s: path loss exponent on the link between jth BS and UE m.
- X_j: Gaussian random variable modeling the shadow fading on the link between jth BS and UE m, with zero mean and $\sigma^2_{X_j}$ variance in db.
- $d_{mb}(j)$: distance between jth BS and UE $m = \sqrt{[r_m^2 + r_b(j)^2 - 2r_m r_b(j)\cos(\theta_m - \theta_b(j))]}$.

The received interference power from the jth interfering BS will be

$$I_j^r = P_j^t G_b G_m C_j d_{mb}(j)^{-\alpha_j} \exp(\beta X_j)$$

which can also be modeled as a random variable in the form of $Y = exp(X)$ as the transmission power, and thus follows a log-normal distribution and its PDF is given by:

$$f_{I_j^r}(z \mid r_m, \theta_m) = \frac{1}{z\sigma_j\sqrt{2\pi}} \exp\left[\frac{-(\ln z - \mu_j)^2}{2\sigma_j^2}\right] \tag{A.2}$$

where $\mu_j = \ln(P_j^t G_b G_m C_j) - \alpha_j d_{mb}(j))$ and $\sigma_j^2 = \beta^2 \sigma^2_{X_j}$

To calculate the background noise value N_{bg}:

- k: the Boltzmann constant.
- T: the ambient temperature in Kelvin.
- W: channel bandwidth.
- φ: Noise figure of the UE.

Therefore $N_{bg} = kTW\varphi$ which can also be represented as a log-normal random variable with a zero variance and mean $\mu_n = \ln(kTW\varphi)$ as follows

$$N_{bg} = \exp(\ln(kTW\varphi) + X_n) \tag{A.3}$$

given that X_n is a Gaussian random variable with zero mean and zero variance [20].

Using three log-normal random variables in equations (A.1, A.2 and A.3), the downlink SINR of UE m is denoted by

$$\gamma_m = \frac{P_s^r}{\sum_{i=1}^{L} I_j^r + N_{bg}} = \frac{P_s^r}{\Upsilon} \tag{A.4}$$

where Υ is the summation of all interference powers and background noise power, and can also be approximated as a log-normal random variable [20].

The PDF of Υ conditioned on the location of UE m is

$$f_\Upsilon(z \,|\, r_m, \theta_m) = \frac{1}{z\sigma_\Upsilon\sqrt{2\pi}} \exp\left[\frac{-(\ln z - \mu_\Upsilon)^2}{2\sigma_\Upsilon^2}\right] \tag{A.5}$$

$$\text{where } \sigma_\Upsilon^2 = \ln\left[\frac{\sum_{j=1}^{L+1} \exp\left(2\mu_j + \sigma_j^2\right)\left(\exp\left(\sigma_j^2\right) - 1\right)}{\left[\sum_{j=1}^{L+1} \exp\left(\mu_j + \frac{\sigma_j^2}{2}\right)\right]^2} + 1\right],$$

$$\mu_\Upsilon = \ln\left[\sum_{j=1}^{L+1} \exp\left(\mu_j + \frac{\sigma_j^2}{2}\right)\right] - \frac{\sigma_\Upsilon^2}{2}$$

Equations A.1, A.5 and A.4 are used to generate the SINR experienced for all UEs, by repeating the same steps for all UEs at all cells.